T-3323

PETROGENESIS AND TECTONIC IMPLICATIONS FOR ARCHEAN MAFIC AND ULTRAMAFIC MAGMAS IN THE ELMER'S ROCK GREENSTONE BELT, LARAMIE RANGE, WYOMING

by

Suzanne M. Smaglik

T-3323

A thesis submitted to the Faculty and the Board of Trustees of the Colorado School of Mines in partial fulfillment of the requirements for the degree of Master of Science (Geochemistry)

Golden, Colorado

Date 30 July 87

Signed: _____
Suzanne M. Smaglik

Approved: _____
E. Craig Simmons
Thesis Co-advisor

Approved: _____
Gregory S. Holden
Thesis Co-advisor

Golden, Colorado

Date July 31, 1987

_____ for GHK
George H. Kennedy
Head, Department of
Chemistry and Geochemistry

ABSTRACT

The Elmer's Rock Greenstone Belt is located in the Laramie Range of southeastern Wyoming, north of the Cheyenne Belt, in the Archean Wyoming Province. This small belt, approximately ten square miles (15 sq. km.), is dominated by metamorphosed mafic and ultramafic volcanic rocks with tholeiitic and komatiitic affinities. Pillow lavas are preserved in the tholeiitic layers but all primary mineralogy and textures have been destroyed by amphibolite grade metamorphism. Also present within the belt are metamorphosed gabbros and several sedimentary rock types. There are few intermediate or felsic volcanics preserved.

Chemical compositions of amphibolites collected in the northwestern portion of the belt suggest four distinct meta-igneous rock types in that area; komatiites, komatiitic basalts, tholeiites and gabbros. Rocks with komatiitic affinities are high in MgO (14-31%) and have hypersthene in the norm. All but two, which are quartz normative, also have normative olivine. Mg numbers range from 70 to 85. They are unlike most Archean ultramafic magmas in that they are slightly higher in SiO_2 and are strongly enriched in incompatible elements (IE) such as Ti, Zr and light rare earth elements (LREE). Those interpreted to be komatiitic basalts are LREE enriched (up to 100 xCHON) and

have highly fractionated chondrite normalized patterns. An ultramafic komatiite is also LREE enriched (2-4 xCHON). Other ultramafic rocks have chondrite normalized REE patterns suggestive of cumulates. The tholeiitic rocks have typical basaltic compositions, Mg numbers of approximately 50 and chondrite normalized REE patterns (5-20 xCHON) which are flat to slightly LREE depleted and flat to heavy REE (HREE) depleted. Most have normative hypersthene and quartz. Two are olivine and hypersthene normative. The gabbroic rocks are much coarser grained than the tholeiites and have higher Al_2O_3 and CaO with Mg numbers between 65 and 70 . All are hypersthene normative with either olivine or quartz. The REE patterns of two gabbros are flat to slightly HREE depleted (5-10 xCHON) with comple entary Eu anomalies. An unusual garnetiferous amphibolite is high in SiO_2, contains almost no MgO and is enriched in iron (Mg number = 15). It has a flat REE pattern (50xCHON) with small negative Ce and Eu anomalies. It is enriched in Zr and Nb and contains no Cr.

The petrogenetic interpretations for these rocks are based on the assumption that the rock compositions are primary and have not been significantly altered by subsequent metamorphism. The komatiite rocks with LREE enriched patterns can be related to each other by different degrees of

pseudo-eutectic partial melting of the same LREE enriched chondritic source. Fractional crystallization of this liquid can account for one of the komatiitic basalts. All but one of the tholeiitic rocks can be related by different degrees of partial melting of a depleted chondritic source in the stability field of garnet with subsequent fractional crystallization prior to eruption as suggested by the Mg numbers which are evolved from a primitive source. One tholeiite, which is higher in MgO and is slightly LREE enriched, may be a mixture of komatiitic and tholeiitic liquids. The gabbros probably represent both orthocumulate and residual liquid from an original liquid in a shallow level magma chamber. The garnetiferous amphibolite may be the result of volcanogenic exhalatives or reworking of adjacent volcanic rocks in an aqueous environment, or may be a less mafic type of metaigneous rock.

The differences between tholeiites and komatiites are one of incompatible element enrichment and degree of melting. The komatiites may have originated from 1) a previously metasomatized portion of the mantle at a depth where garnet is a stable phase or 2) where eclogite is formed or 3) the melt may have been contaminated by crus tal material during ascent. The source of the tholeiites began melting in a depleted portion of the mantle at a

depth where garnet begins to become unstable. The depths at which the two sources began to melt may be similar.

A reasonable tectonic environment for the formation of these rocks is one in which rising diapirs and near surface magma chambers exist. Such features would be expected where the crust was thin, such as divergent environments, or in a melting zone above subducted lithosphere in a zone of convergence. The lack of an extensive alkali basalt suite and the interlayering of clastic sediments with the volcanics suggests a primitive zone of convergence, such as the Archean equivalent of an island arc or continental margin.

TABLE OF CONTENTS

LIST OF FIGURES

Page

LIST OF TABLES

ACKNOWLEDGEMENTS

I would like to thank Greg Holden for introducing me to the area and for help with field mapping, sample collection and numerous discussions. Craig Simmons provided instruction on the use of the mass spectrometer and help with data interpretation. I would like to thank the other members of my committee, Steve Daniel and George Snyder, for their encouragement and support. Tom Light of the USGS, provided limited financial support and part-time employment for four years. I gratefully acknowledge Zell Peterman of the USGS for use of the x-ray and mass spectrometers and Loretta Kwak of the USGS for her help and support in analyzing the REE. I would especially like to thank Ken Sims and Nate Bower of The Colorado College for their help with transition metal analysis and Department of Geology for the use of their XRF machine. Thanks also go to Tom Musselman for his computer programs and help with other computer related problems. I would also like to thank my partner Warren Ulmer, who was helpful in collecting and preparing samples for analyses, for his patience while I completed my work.

DEFINITIONS OF SYMBOLS USED

ERGB	Elmer's Rock Greenstone Belt
IE	incompatible element
REE	rare earth element(s)
LREE	light REE (Ce - Nd)
MREE	middle REE (Sm - Gd)
HREE	heavy REE (Dy - Yb)
x CHON	times chondrite values
Eu*	the difference between the true Eu_N and that interpolated between Sm_N and Gd_N
N	chondrite normalized value
Ga	billion years
XRF	x-ray fluorescence
LOI	loss on ignition
Mg number (#)	$[MgO]/[MgO+FeO_T]$ x 100
FeO_T	total iron calculated as FeO
CIPW	hypothetical mineral assemblage
dpl	depleted
enr	enriched
plag	plagioclase
cpx	clinopyroxene
opx	orthopyroxene
ol	olivine

OFB	ocean floor basalt
IAT	island arc tholeiite
C_L	concentration of element in the liquid
C_o	initial concentration of element
F	amount of melting or liquid remaining (%)
D_o	bulk solid-melt distribution coefficient
X_i	amount of element in a single phase
Kd	single element distribution coefficent
X_L	amount of liquid in orthocumulate
X_s	amount of solids in orthocumulate
C_s	concentration of element in cumulate solids
$3xH_2O$	triply distilled water

INTRODUCTION

Petrogenetic studies of Archean greenstone belts provide keys to discovering the early evolution of the earth. Archean greenstone belts are elongated, synformal aggregates of supracrustal volcanics and sediments surrounded by older gneissic basement. Greenstone belt stratigraphy is dominated by basal mafic volcanics, including komatiites, komatiitic basalts, tholeiites and pillow lavas, which are overlain by and interbedded with sedimentary rocks such as greywacke, conglomerate containing granitic clasts in a greywacke matrix, pelite, marble, banded iron formation and minor quartzite. Structural features include steep regional dip, bedding parallel schistosity, curvelinear axial fold traces, branching synclines, highly strained boundaries with the surrounding granitic-gneiss terrain and strike faults along the synclines. Other features common to greenstone belts include mafic schlieren and mafic and ultramafic dikes in the bordering gneisses, sulfides present in the metavolcanics and often a metamorphic grade higher at the edges than in the center of the belt (Anhauesser, et al, 1969).

Petrogenetic studies of greenstone belt rocks have focused mainly on the genetic relationship between the komatiitic and tholeiitic rocks. Komatiites are consid-

ered to be generated at great depths (>100 km) by up to 60 percent batch melting or by lower percentages of melting by continuous or sequential melting of the mantle (Arndt, 1977; Cox, 1978; Sun & Nesbitt, 1978; Nesbitt, et al, 1979; Jaques & Green, 1980; Huppert & Sparks, 1980; Ohtani, 1984). Komatiitic basalts may be the result of differentiation of komatiitic magmas or lower percentages of melting at greater depths (Jaques & Green, 1980; Hanson, 1981; Nisbet & Chinner, 1981). Tholeiites may have formed from different sources than the komatiites, at lower percentages of melting at shallower depths, or by differentiation of komatiitic liquids at crustal levels (Jaques & Green, 1980; Sun & Nesbitt, 1978).

Geochemical data have been used to set limits on the tectonic setting of these rocks. Most models are developed by comparing the trace element chemistry of the greenstone rocks to volcanic rocks found in modern orogenic settings (Hart, et al, 1970; Jahn, et al, 1974; Condie, 1976a, 1986). Caution must be exercised when using these comparisons as the conditions of formation and tectonic framework of post-Archean rocks may not be equivalent to those of Archean rocks.

Opinions on the chemical variations in rocks derived from melting of the upper mantle composition during

Archean time vary from a heterogeneous mantle to contamination of magma by older sialic crust. Subtle differences between element ratios of different greenstone belts are often interpreted to represent differences in source compositions (Gast, 1968; Glikson, 1971; Nesbitt, et al, 1979; Sun, et al, 1979; Smith & Erlank, 1982; Sun, 1984). However, as more evidence is gathered, some of these variations have been attributed to crustal contamination (Huppert & Sparks, 1985a, 1985b; Barley, 1986). Isotopes may be the most useful tool in distinguishing these two phenomena (Barley, 1986; Sun, 1984).

Mafic and ultramafic Archean rocks of the Wyoming Province have not been studied in great detail (Condie, 1976b). The Wyoming Province is the westernmost extent of the Archean North American craton. Most of the studies of this craton have concentrated on Canadian greenstone belts. Our study of the ERGB should provide information on the magma generation processes which occurred during the formation of the belt and allow us to compare the formation of this belt with that of greenstone belts within other cratons.

GENERAL GEOLOGY

The Elmer's Rock Greenstone Belt is one of several small greenstone belts which occur within the Archean Wyoming Province of North America (Condie, 1976b). Unfortunately, only fragments of these belts are exposed within the province because of post-depositional tectonics and erosion, which makes correlation between the belts and interpretation of the Archean tectonic history of the province difficult. The ERGB is located in the Laramie Range, approximately twenty miles to the north of the Cheyenne Belt which separates the Archean Wyoming Province from the Proterozoic eugeoclinal terrain to the south (Fig.1). Details of the geology of this belt are reported in Graff et al, 1982 and Snyder, 1984.

The ERGB possesses the necessary stratigraphic and structural features of a greenstone belt as described in the section above. Figure 2 shows a simplified geologic map of the belt. The dominant structure of the belt is an east-west trending synform (Graff, et al, 1982). Metamorphosed mafic volcanic rocks with ultramafic pods and sedimentary layers dominate the belt, which overlies a granitic-gneiss basement. The belt has been intruded to the east by granite with gneissic inclusions and to the south by syenite. Metamorphosed ultramafic pods and sedimentary

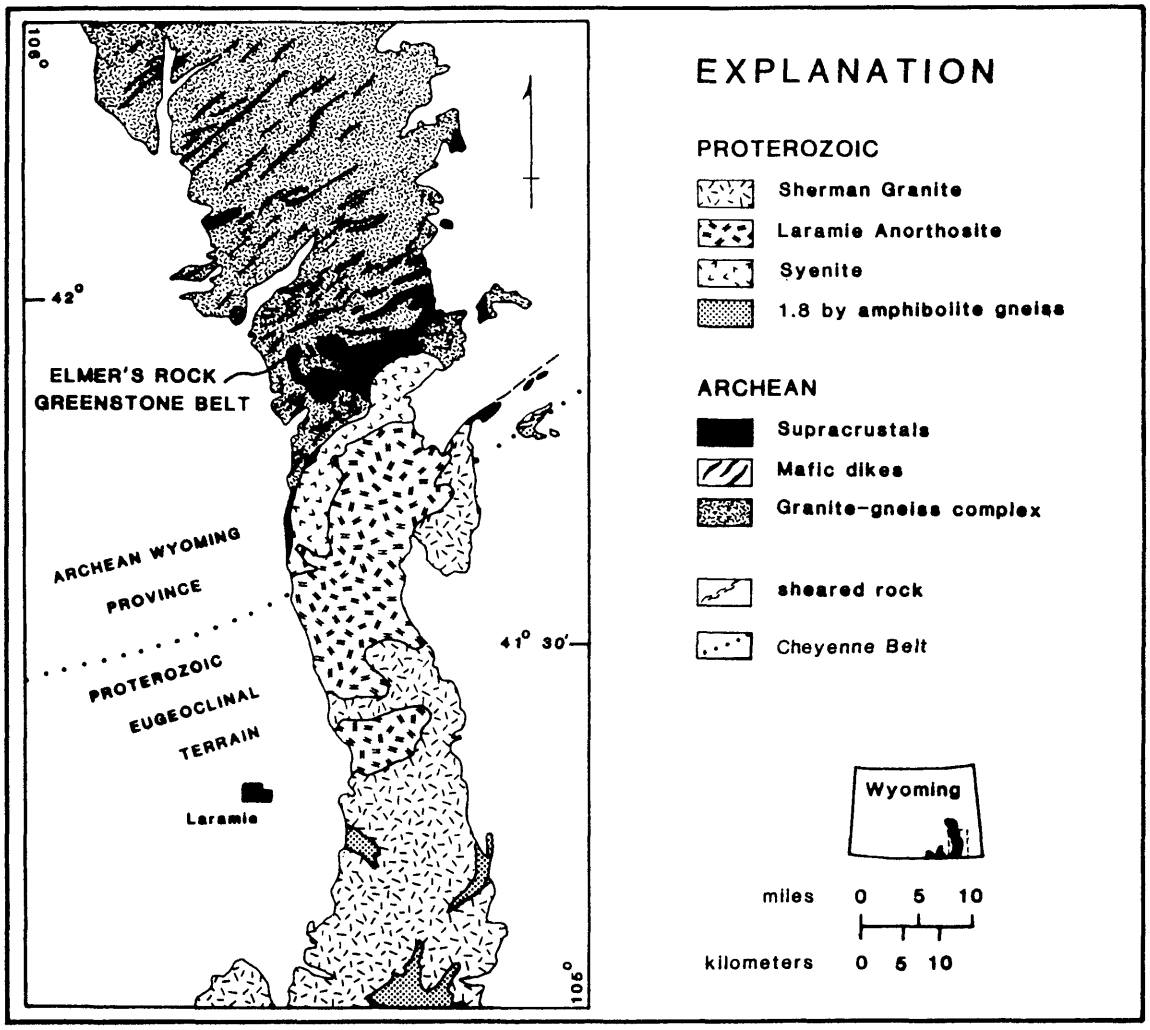

Figure 1.--Location of the Elmer's Rock Greenstone Belt in relation to Precambrian rocks of the Laramie Range, southeastern Wyoming (adapted from Graff, et al, 1982).

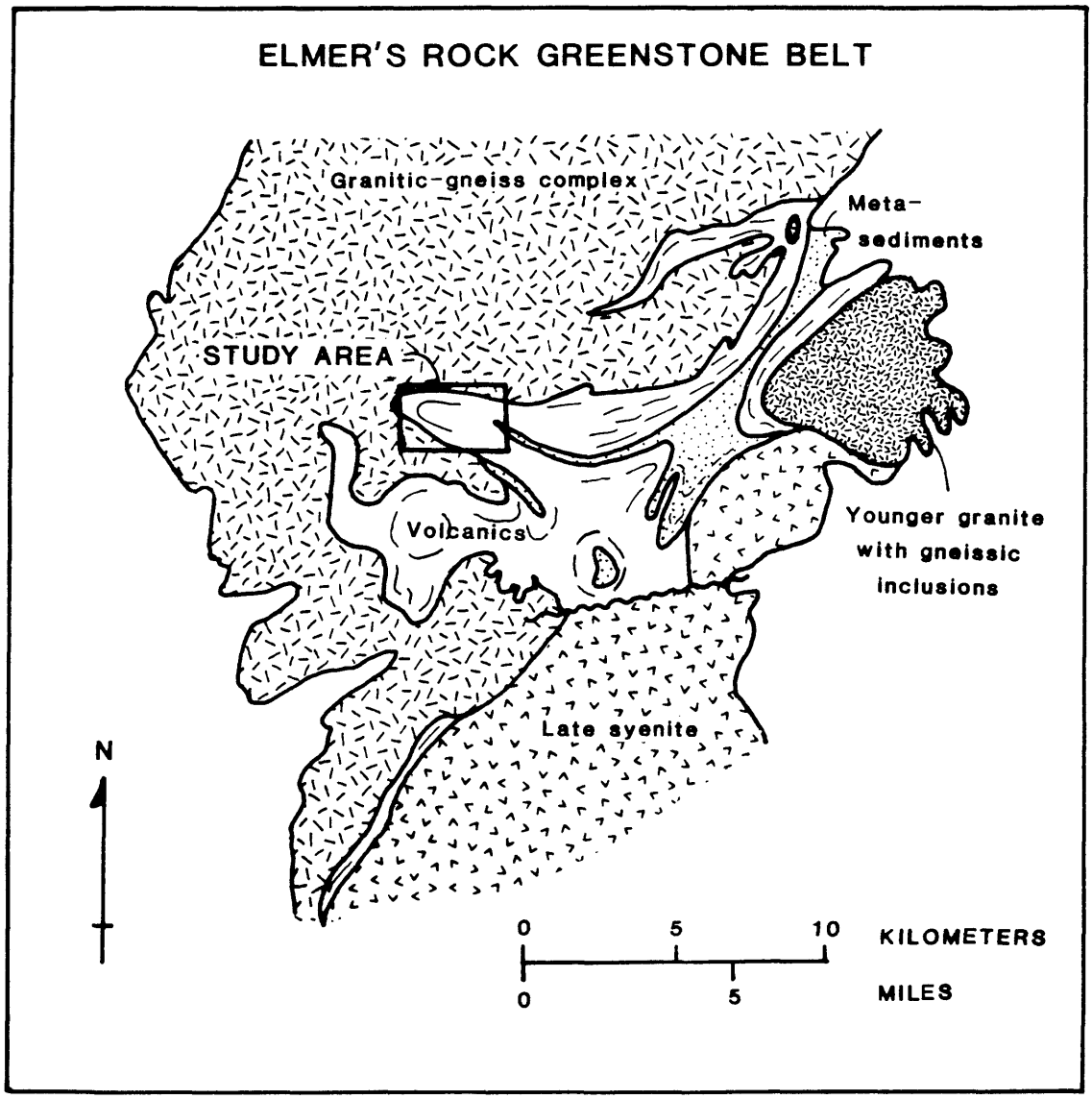

Figure 2.--Simplified geologic map of the Elmer's Rock Greenstone Belt indicating study area (adapted from Graff, et al, 1982).

rocks occur within the mafic volcanics. The age of the belt is not well known. The granitic-gneiss complex is dated between 2.9 and 3.2 Ga (Peterman and Hildreth, 1977) and the younger intrusives which contain gneissic inclusions are dated at 2.5-2.6 Ga (Hills and Armstrong, 1974).

The focus of this study is the metavolcanic rocks in the northwestern portion of the ERGB. The synform is most evident in this part of the belt where the most extensive exposure of metavolcanic rocks can be found. The geology and sample locations are shown in Fig. 3. The major rock types in this portion of the belt are (1) fine-grained mafic amphibolite, (2) fibrous ultramafic amphibolite, (3) coarse-grained mafic amphibolite, (4) garnet-bearing amphibolite and (5) metamorphosed sediments. Felsic volcanics and banded iron formation do not occur within this portion of the belt.

The mineral assemblages found in all of these rocks suggest metamorphism to amphibolite grade. When rocks of basaltic composition, that is, a rock containing plagioclase, augite and olivine or hypersthene, are subjected to high pressure and temperatures under slightly hydrous (<5% H_2O) conditions, the result is usually an amphibolite consisting of plagioclase and hornblende $\pm$ garnet. Ultramafic igneous rocks composed of olivine and pyroxene

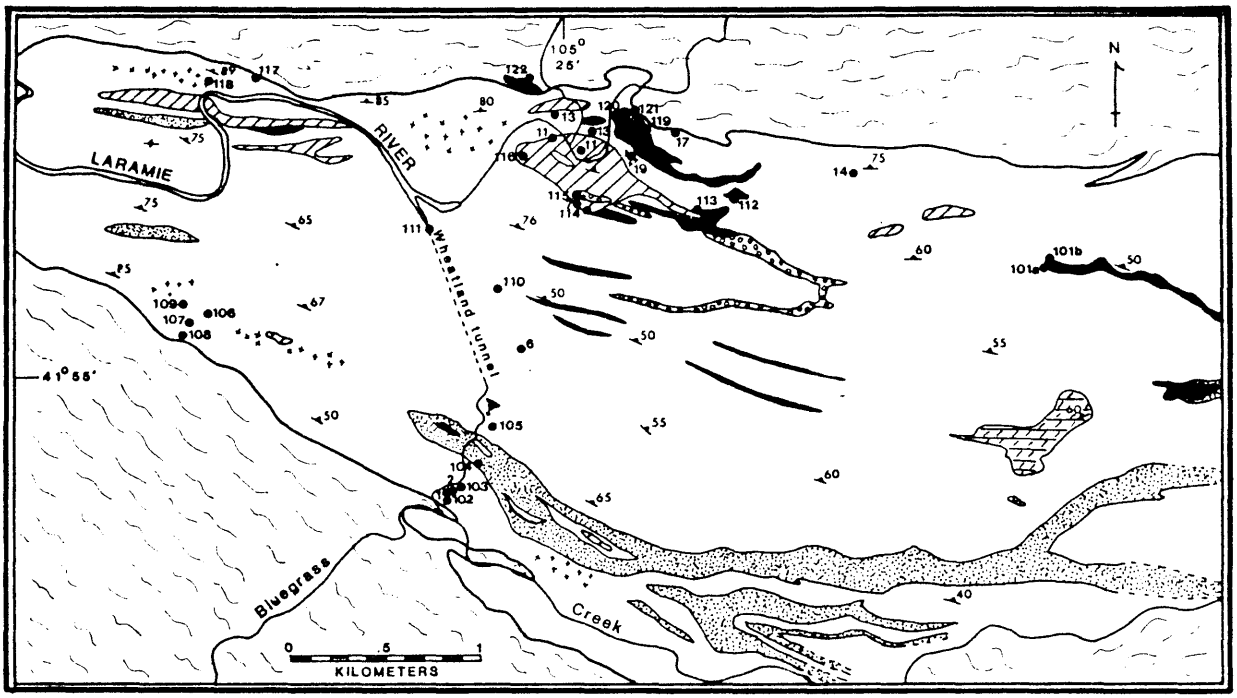

Figure 3.--Detailed geologic map of the study area in the northwestern portion of the Elmer's Rock Greenstone Belt. Sample locations are indicated by circles; numbers correspond to those in the text minus their prefix (ER).

become actinolite/chlorite schists under hydrous high pressure and temperature conditions (Winkler, 1979). These mineral assemblages are found in the ERGB rocks. Detailed petrography of the rocks collected for this study is given in Appendix II.

The fine-grained mafic amphibolite is the dominant rock type in the belt. It occurs in discreet layers which have a strong foliation, the dip of which increases from south to north through the belt. Pillow structures are locally preserved within this unit near the southern edge of the synform, although many have been deformed beyond recognition. These rocks are composed of approximately equal portions of amphibole and plagioclase with accessory sphene and in some, quartz. The amphibole in these rocks is either green hornblende, anthophyllite or both. The composition of the plagioclase is andesine. Accessory minerals such as apatite, hematite and opaques are common. One sample also has accessory biotite.

The fibrous ultramafic amphibolite is the least abundant rock type in the belt. It occurs as lenticular pods and folded layers within the fine-grained mafic amphibolite layers. The fibrous ultramafic amphibolites consist mainly of tremolite/actinolite and chlorite with accessory opaques. A few samples also contain anthophyllite or cum-

mingtonite and one contains accessory plagioclase and biotite.

The coarse-grained mafic amphibolite has previously been mapped in the same unit as the fine-grained mafic amphibolite (Graff et al, 1982; Snyder, 1984) but this study distinguishes it as a separate unit because of its texture and field relationships. It consists of amphibole, plagioclase and accessory opaques. The amphiboles are green hornblende and cummingtonite. The plagioclase is andesine. One sample contains quartz and one has accessory sphene. The contact between this unit and the fine-grained unit is gradational. The coarse-grained unit does not posess distinct layers and cross cuts layers in the fine-grained unit. It occurs mainly in the northern portion of the synform but pods can be found within the fine-grained amphibolite layers in other parts of the belt.

Throughout the main body of the belt, occurrences of fine-grained disseminated garnet can be found. They occur within what appeared to be layers of fine-grained mafic amphibolite but can be traced for only short distances. This garnet bearing amphibolite was originally mapped with the fine-grained amphibolite unit, but its chemical composition and mineralogy suggest that it may be an entirely different unit and that it may be of volcanogenic-

sedimentary origin. This garnet amphibolite consists of blue-green hornblende, quartz, almandine garnet, andesine and iron oxides.

The metamorphosed sediments, mainly greywacke in composition, occur as folded beds within the other units. The metasediments are composed mainly of quartz and plagioclase with biotite and hornblende or chlorite and sericite. Garnet, zircon and/or apatite appear as accessory minerals in some rocks. The metaconglomerate contains sizable clasts of granitic material in a greywacke matrix.

An attempt was made to map individual flows within the mafic amphibolite. The post-depositional tectonics and metamorphism have made this very difficult. The sample locations were chosen stratigraphically across and along the belt so that any chemical variation in these two directions could be noted. Although the main focus of this study is the metavolcanic rocks of the belt, several metasediments were also collected to give some clue as to the tectonic environment in which the volcanic rocks were erupted.

ANALYTICAL METHODS

The data presented in this thesis are from two sets of samples collected in the area. Those with labels ER-XX were collected by G. Holden in 1983 and those with labels ER1XX were collected by G. Holden and S. Smaglik in 1984.

The ER1XX suite was prepared and analyzed by S. Smaglik. Homogenized splits of these samples in the ER1XX set were pulverized to -200 mesh grain size and analyzed for major and trace elements. Detailed descriptions of the analytical procedures used can be found in Appendix I.

Major elements were determined by x-ray fluorescence (XRF) spectrometry using fused glasses on a Rigaku 3080E XRF spectrometer at the Colorado School of Mines, Golden, CO. Analytical uncertainties were determined using duplicates and standards and range between 1 and 5 percent for these elements. Total iron was reported as Fe_2O_3. The iron as FeO was determined using the wet chemical method of Goldich, 1984.

The trace elements Rb, Sr, Y, Nb and Zr were determined using loose powder and mylar film (Spex Industries) on a Kevex 5100 X-ray energy spectrometer at the U.S. Geological Survey, Branch of Isotope Geology (USGS,BIG) Denver, CO. The trace elements Co, Cr and V were determined using fused glasses on a Rigaku 3070 XRF spectrometer at

The Colorado College, Department of Geology, Colorado Springs, CO. The analytical uncertainties for all of the trace elements were estimated at less than 10 percent.

Loss on ignition (LOI) was determined by gravimetric difference, taking into account the change in weight due to the oxidation of iron. Analytical uncertainty was estimated at less than 2 percent.

Eight rare earth elements (REE) were determined by isotope dilution at the USGS, BIG, using a 12" radius NBS Shields-type mass spectrometer. The chemical separation procedure used was a modified version of that described by Lambert (1982) The separations were performed at the Colorado School of Mines. The analytical uncertainty for the REE analyzed is less than 2 percent.

The ER-XX set of samples were analyzed for major and trace elements by chemists at the Pennsylvania State University, by atomic absorption methods. The analytical uncertainty was estimated at less than 5 percent. The iron as FeO was determined using the method of Goldich, 1984.

ANALYTICAL RESULTS

The analytical results of major and trace element analyses and calculated norms of the samples collected in this belt are presented in Table 1. The REE abundances of selected samples are given in Table 2.

It is assumed that the major elements in these rocks, except for sodium and potassium, were not significantly mobilized during metamorphism subsequent to eruption. Beswick (1982) has shown this to be true for rocks of komatiitic composition. Ernst (1987) used oxygen isotope studies to conclude that the major elements and mineralogy of Permo-Triassic mafic and ultramafic metavolcanics from the Klamath Mountains were not significantly affected by interaction of seawater during regional metamorphism. The consistency of the major elements, except Na and K, in rocks collected from the ERGB, especially between the two different collection suites, supports our assumption that the analytical results represent the original compositions. Sodium, K and P are in such low abundances in these rocks that they are near the detection limit for the analytical method, which may explain some of the scatter for these elements. Therefore they will not be used in our petrogenetic interpretations.

Most petrogenetic interpretations of metamorphosed

TABLE 1.

Major and trace element analyses and CIPW norms for rocks from the Elmer's Rock Greenstone Belt.

Komatiitic rocks

Sample #	ER101b	ER122	ER113	ER112	ER119	ER101a
%						
SiO_2	51.71	51.17	45.16	51.57	48.01	51.04
TiO_2	0.21	0.78	1.77	0.21	0.41	0.10
Al_2O_3	4.80	4.57	7.75	5.72	9.36	5.17
Fe_2O_3	0.80	0.70	2.45	0.72	1.19	1.47
FeO	6.92	8.17	12.69	9.40	8.68	7.34
MnO	0.09	0.11	0.22	0.20	0.20	0.11
MgO	20.56	20.75	16.39	20.79	16.76	23.20
CaO	11.15	10.61	8.74	7.45	11.48	8.36
Na_2O	0.13	0.17	0.76	0.17	0.37	0.00
K_2O	0.06	0.06	0.14	0.06	0.11	0.04
P_2O_5	0.02	0.09	0.24	0.01	0.03	0.02
LOI	2.97	2.76	2.80	2.38	2.20	3.01
TOTAL	99.41	99.93	99.11	98.66	98.80	99.95
Mg #	84.12	81.91	69.71	79.77	77.49	84.93
FeO_T	7.64	8.80	14.89	10.05	9.75	8.66
Cr (ppm)	3120	1024	1157	2102	1169	3395
Co	72	47	85	69	62	77
V	110	161	267	153	169	101
Rb	3	0	6	3	4	3
Sr	8	4	21	7	27	6
Y	3	11	16	2	14	3
Zr	11	69	171	8	46	14
Nb	0	6	31	1	1	0
Q	0.06	--	--	0.65	--	--
C	--	--	--	--	--	--
or	0.35	0.36	0.87	0.34	0.65	0.23
ab	1.14	1.45	6.65	1.48	3.22	--
an	12.80	11.88	17.99	15.25	24.42	14.44
di	35.36	33.19	20.52	18.49	27.54	22.36
hy	48.71	48.37	31.22	62.27	32.10	57.33
ol: fo	--	1.53	9.95	--	6.78	2.44
ol: fa	--	0.43	5.04	--	2.62	0.56
mt	1.20	1.05	3.69	1.08	1.79	2.19
il	0.33	1.52	3.50	0.41	0.80	0.38
ap	0.04	0.22	0.58	0.02	0.08	0.05

TABLE 1 (con't).

Komatiitic rocks

Sample #	ER121	ER-14	ER-15	ER-17	ER-19	ER107
%						
SiO_2	50.22	48.80	45.70	45.30	43.00	49.56
TiO_2	0.29	0.78	0.42	0.38	0.29	0.88
Al_2O_3	6.72	10.10	8.30	8.50	7.20	11.96
Fe_2O_3	0.78	1.34	1.37	0.41	3.21	1.87
FeO	8.18	10.28	13.05	9.22	6.21	9.31
MnO	0.18	0.20	0.18	0.18	0.19	0.18
MgO	20.42	13.70	20.00	22.70	28.40	11.20
CaO	8.38	10.30	5.78	7.02	3.13	10.41
Na_2O	0.12	1.36	0.33	0.26	0.03	1.65
K_2O	0.07	0.19	0.05	0.03	0.01	0.30
P_2O_5	0.02	0.05	0.06	0.04	0.06	0.08
LOI	0.95	1.93	4.01	4.92	7.36	1.86
TOTAL	96.33	99.03	99.25	98.96	99.09	99.25
Mg #	81.65	72.66	75.73	84.06	89.07	68.19
FeO_T	8.88	11.48	14.28	9.59	9.10	10.99
Cr (ppm)	1762	1250	2050	850	4900	713
Co	65	70	55	84	106	54
V	156	255	205	130	120	282
Rb	0	7	4	3	4	6
Sr	8	76	13	14	32	93
Y	4	19	24	16	12	10
Zr	20	43	29	40	45	48
Nb	0	--	--	--	--	1
Q	--	--	--	--	--	--
C	--	--	--	--	1.74	--
or	0.42	1.15	0.31	0.19	0.06	1.84
ab	1.05	11.84	2.93	2.34	0.28	14.30
an	18.47	21.49	22.03	23.28	16.50	24.86
di	19.94	24.74	6.11	10.65	--	24.06
hy	57.29	29.88	49.18	38.67	49.06	27.43
ol: fo	0.78	3.76	9.76	16.79	23.39	2.01
ol: fa	0.24	1.63	3.88	3.94	3.14	1.15
mt	1.19	3.81	4.82	3.28	5.07	2.78
il	0.58	1.52	0.84	0.77	0.60	1.70
ap	0.06	0.12	0.15	0.10	0.15	0.18

TABLE 1 (con't).

Tholeiities

Sample #	ER117	ER102	ER110	ER106	ER105	ER103
%						
SiO_2	50.83	50.14	50.29	50.03	49.75	50.98
TiO_2	1.92	1.68	1.31	1.01	0.92	0.91
Al_2O_3	14.68	14.24	13.72	13.54	14.09	13.89
Fe_2O_3	2.52	2.13	3.22	1.78	1.95	1.34
FeO	10.47	10.13	9.76	10.70	10.53	9.75
MnO	0.19	0.19	0.20	0.21	0.17	0.19
MgO	5.64	6.47	6.76	6.99	7.48	7.65
CaO	10.40	10.50	10.78	10.45	10.70	11.62
Na_2O	2.19	2.54	2.13	1.70	1.70	1.42
K_2O	0.19	0.25	0.28	0.25	0.26	0.26
P_2O_5	0.16	0.14	0.12	0.09	0.08	0.08
LOI	1.17	1.51	1.17	2.17	2.06	1.14
TOTAL	100.36	99.92	99.74	98.90	99.69	99.20
Mg #	48.98	53.23	55.23	53.79	55.88	58.31
FeO_T	12.74	12.05	12.66	12.30	12.28	10.96
Cr (ppm)	94	179	254	192	245	110
Co	48	49	45	52	50	46
V	372	356	305	308	290	282
Rb	7	13	8	4	8	11
Sr	143	142	139	101	94	117
Y	22	20	15	150	16	14
Zr	93	79	56	49	50	45
Nb	3	2	1	1	3	2
Q	5.14	1.44	3.46	4.00	2.42	4.33
C	--	--	--	--	--	--
or	1.11	1.47	1.68	1.50	1.57	1.57
ab	18.72	21.81	18.26	24.84	14.72	12.21
an	29.89	27.19	27.44	29.56	30.80	31.39
di	16.95	21.23	21.36	19.34	18.97	22.05
hy	19.96	20.94	20.24	25.89	26.65	24.53
ol: fo	--	--	--	--	--	--
ol: fa	--	--	--	--	--	--
mt	3.69	3.14	4.74	2.66	2.89	1.98
il	3.67	3.24	2.52	1.98	1.79	1.75
ap	.38	0.33	0.28	0.22	0.19	0.19

TABLE 1 (con't).

Tholeiites

Sample #	ER108	ER109	ER111	ER-1	ER-2	ER-6
%						
SiO_2	50.10	50.27	52.10	50.20	50.70	50.30
TiO_2	1.46	0.62	0.78	0.76	0.75	1.12
Al_2O_3	13.28	15.51	12.13	14.20	14.60	14.80
Fe_2O_3	2.33	1.72	1.70	1.35	1.38	1.61
FeO	11.44	7.82	8.94	9.49	9.15	10.34
MnO	0.20	0.17	0.18	0.22	0.19	0.20
MgO	6.11	7.27	9.11	7.63	7.97	7.00
CaO	11.15	10.78	10.96	12.70	11.10	10.80
Na_2O	2.03	2.64	1.47	1.72	2.25	2.42
K_2O	0.31	0.25	0.47	0.15	0.31	0.18
P_2O_5	0.13	0.06	0.07	0.09	0.07	0.12
LOI	1.27	2.07	1.00	1.18	1.13	1.13
TOTAL	99.82	99.18	98.90	99.69	99.60	100.02
Mg #	48.78	62.37	64.49	58.90	60.83	54.69
FeO_T	13.54	9.37	10.47	10.70	10.39	11.79
Cr (ppm)	139	36	454	400	330	280
Co	62	54	50	50	50	52
V	344	249	263	270	255	310
Rb	9	5	8	11	7	8
Sr	107	126	116	88	105	127
Y	21	9	11	17	21	22
Zr	67	28	45	43	40	61
Nb	4	1	3	--	--	--
Q	3.65	--	4.84	1.14	--	0.07
C	--	--	--	--	--	--
or	1.89	1.50	2.81	0.90	1.86	1.08
ab	17.85	22.95	12.68	14.77	19.33	20.17
an	26.78	30.49	25.68	31.04	29.27	29.31
di	20.93	21.15	23.94	26.55	21.45	19.86
hy	22.60	17.93	25.56	21.92	23.88	24.71
ol: fo	--	1.20	--	--	0.31	--
ol: fa	--	0.89	--	--	0.25	--
mt	3.46	2.56	2.52	1.99	2.03	2.36
il	2.83	1.20	1.51	1.47	1.45	2.15
ap	0.30	0.14	0.17	0.21	0.16	0.28

TABLE 1 (con't).

Tholeiites	Gabbros				
Sample #	ER-13	ER114	ER116	ER-7	ER-11
%					
SiO_2	49.80	52.05	46.49	50.50	49.30
TiO_2	0.86	0.77	0.58	0.57	0.58
Al_2O_3	14.50	12.14	15.55	17.00	17.20
Fe_2O_3	1.54	3.63	0.86	1.62	1.00
FeO	10.46	7.42	9.48	7.12	6.97
MnO	0.20	0.18	0.19	0.16	0.15
MgO	6.97	9.06	11.76	7.86	7.63
CaO	11.30	10.94	10.10	11.10	12.50
Na_2O	2.35	1.48	1.61	2.15	2.20
K_2O	0.18	0.46	0.19	0.14	0.47
P_2O_5	0.08	0.07	0.05	0.07	0.05
LOI	1.18	1.40	1.73	1.09	1.68
TOTAL	99.42	99.60	98.57	99.38	99.73
Mg #	54.29	68.53	68.85	66.31	66.12
FeO_T	11.84	10.69	10.25	8.58	7.87
Cr (ppm)	220	639	157	640	740
Co	54	48	68	43	40
V	285	142	213	230	215
Rb	5	6	8	5	19
Sr	128	141	119	156	152
Y	21	14	9	15	14
Zr	50	47	31	29	32
Nb	--	2	1	--	--
Q	--	6.85	--	1.07	--
C	--	--	--	--	--
or	1.08	2.76	1.13	0.84	2.83
ab	20.24	12.75	14.04	18.51	18.99
an	28.99	25.59	35.81	36.95	36.38
di	22.76	23.52	12.68	15.12	21.59
hy	20.57	21.50	15.56	23.85	9.77
ol: fo	1.07	--	11.37	--	4.67
ol: fa	1.15	--	6.88	--	3.06
mt	2.27	5.36	1.29	2.39	1.48
il	1.66	1.49	1.13	1.10	1.12
ap	0.19	0.17	0.11	0.17	0.12

TABLE 1 (con't).

Metasediments

Sample #	ER118*	ER104	ER120
%			
SiO_2	59.21	67.63	65.99
TiO_2	1.46	0.94	0.52
Al_2O_3	10.12	14.53	16.62
Fe_2O_3	6.50	0.28	0.47
FeO	11.15	4.43	3.42
MnO	0.26	0.08	0.04
MgO	1.36	3.30	2.21
CaO	5.52	2.78	1.68
Na_2O	2.55	2.92	5.91
K_2O	0.30	2.34	0.33
P_2O_5	0.45	0.12	0.10
LOI	1.54	1.52	2.03
TOTAL	100.42	100.87	99.32
Mg #	15.18	57.07	31.87
FeO_T	16.99	4.68	3.84
Cr (ppm)	0	24	23
Co	22	21	15
V	94	101	118
Rb	12	62	8
Sr	69	158	103
Y	66	17	7
Zr	262	146	110
Nb	13	6	2
Q	23.87	28.37	16.86
C	--	2.43	3.64
or	1.80	13.89	1.92
ab	21.91	24.88	48.86
an	15.47	13.13	7.53
di	8.14	--	--
hy	19.41	14.83	19.35
ol: fo	--	--	--
ol: fa	--	--	--
mt	5.55	0.40	0.67
il	2.81	1.79	0.96
ap	1.06	0.27	0.22

* protolith of this rock is uncertain

TABLE 2.

Rare earth element contents in samples from the Elmer's Rock Greenstone belt.

Sample #	ER101b	ER122	ER113	ER112	ER119	ER107
ppm						
Ce	2.88	25.52	86.26	1.77	14.51	10.26
Nd	1.51	14.74	42.38	1.71	7.50	6.99
Sm	0.40	3.19	7.32	0.53	1.86	2.06
Eu	0.12	1.09	1.94	0.34	1.40	0.77
Gd	0.54	2.85	5.32	0.65	2.16	2.53
Dy	0.60	2.43	3.92	0.76	2.48	2.66
Er	0.39	1.26	1.78	0.54	1.58	1.45
Yb	0.38	1.13	1.50	0.56	1.63	1.28
REE_T	6.25	52.22	149.43	6.85	33.13	28.02
$(Ce/Yb)_N$	1.93	5.77	14.74	0.81	2.28	2.05
Eu/Eu*	0.83	1.10	0.92	1.80	2.16	1.04

Sample #	ER117	ER102	ER110	ER106	ER105
ppm					
Ce	17.75	16.21	10.12	8.97	8.17
Nd	12.99	11.86	7.64	7.12	6.30
Sm	3.98	3.65	2.38	2.32	2.03
Eu	1.42	1.34	0.90	0.87	0.77
Gd	4.68	4.60	2.98	3.13	2.56
Dy	5.08	5.09	3.28	3.70	3.18
Er	3.12	2.96	1.87	2.35	2.02
Yb	2.47	2.77	1.18	2.37	2.02
REE_T	51.48	48.49	30.89	30.83	27.03
$(Ce/Yb)_N$	1.84	1.50	1.51	0.97	1.04
Eu/Eu*	1.00	1.01	1.05	1.00	1.00

Sample #	ER114	ER116	ER118	ER104	ER120
ppm					
Ce	8.38	4.20	38.18	52.85	46.15
Nd	5.97	2.02	31.03	17.27	15.56
Sm	1.84	0.98	9.96	3.15	2.71
Eu	0.54	0.42	3.24	0.79	0.84
Gd	2.48	1.27	13.10	2.85	2.09
Dy	2.76	1.52	15.32	2.52	1.72
Er	1.70	0.99	9.73	1.39	0.96
Yb	1.65	1.01	9.80	1.38	0.94
REE_T	25.32	13.40	130.37	82.22	70.96
$(Ce/Yb)_N$	1.30	1.07	0.99	9.33	12.53
Eu/Eu*	0.78	1.18	0.88	0.80	1.04

igneous rocks assume that transition metals and REE are essentially immobile during metamorphism. This assumption is not valid for metasomatic changes which occur in the source prior to melting. As more studies are conducted on the effect of metamorphism on the trace element contents of rocks, it is clear that there is no simple relationship between the degree of mobility or immobility and the grade of metamorphism or original rock type (Humphris, 1984; Ludden, et al, 1982; Ludden & Thompson, 1978, 1979; Humphris & Thompson, 1978a, 1978b; Ludden & Humphris, 1978; Condie, et al, 1977).

The REE are thought to be among the most immobile components of rocks and their behavior in the geologic environment, which is governed by the similarity in their size and ionic charge (+3), make them an excellent tool in interpreting the origin of a rock. If the REE are affected by weathering or alteration, the change in composition will be a function of the original abundance in the rock and distribution within the phases, the concentration of REE in the interacting fluid and partitioning between the mineral phases and the fluid, and the ability of the REE released from the original minerals to be accommodated by the secondary minerals which are formed by the alteration processes (Humphris, 1984).

For igneous rocks, the crystallization history and distribution of trace elements among the minerals phases is one of the main controls on the mobility of the REE, and other trace elements, during metamorphism. Each mineral has a typical range for the distribution coefficients (Kd's) of these elements (Henderson, 1984; Hanson, 1980; Allegre & Minster, 1978; Irving, 1978). Many accessory minerals, such as apatite, zircon and sphene, concentrate the REE, and if these minerals are more susceptible to weathering and alteration than the major components of a rock, they will significantly affect the whole rock distribution of the REE (Humphris, et al, 1978).

One exception to this immobility is Eu. Europium occurs in the +2 and +3 ionic states. Europium anomalies are caused by plagioclase accumulation, source characteristics or alteration effects (Sun & Nesbitt, 1978a). Both Eu 2+ and 3+ behave incompatibly during melting (Hanson, 1980). Major mantle minerals have low mineral-melt Kd's for REE, making it unlikely that they would produce a Eu anomaly in the rock (Henderson, 1984; Sun & Nesbitt, 1978a). Cerium can also be affected by alteration, as it occurs in both the 3+ and 4+ states. Oxidation of Ce can produce an anomaly in the rock (Henderson, 1984). Cerium anomalies are not as common as Eu anomalies, however.

Since none of the trace elements in the ERGB rocks show any anomalous variation larger than the analytical uncertainty, we consider them to be of primary igneous origin.

Major Element Chemistry

The most significant component which distinguishes the rock types is MgO. For the mafic and ultramafic volcanic rocks, the MgO content varies from 5 to 31 wt. percent with a gap between 11 and 16 wt. percent. The mafic volcanics have less than 11 wt. percent MgO and generally have normative quartz and hypersthene, although a few are olivine normative. Their Mg numbers are less than 69. The high-Mg ultramafic amphibolites, which have between 16 and 31 wt. percent MgO, are hypersthene and/or olivine normative and have Mg numbers greater than 70. They are slightly higher in SiO_2 than most Archean ultramafic rocks (Basaltic Volcanism Study Project, 1981). The high-Mg rocks are generally lower in Al_2O_3, CaO and TiO_2 than those with lower MgO contents. With three exceptions, the CaO/Al_2O_3 ratios of the Mg-rich rocks are greater than one, while those of the mafic volcanic rocks are less than one. The wt. percent FeO is similar in both rock types. The abundances of alkali elements in these rocks are quite variable and unsystematic, but all are low. The coarse-

grained amphibolites h ave Mg numbers intermediate to those of the fine-grained amphibolite and the ultramafic amphibolite.

The metagreywackes contain less than 4 wt. percent MgO, higher in SiO_2 and are easily distinguished from the metavolcanic rocks. The garnet amphibolite has a SiO_2 content 10 wt. percent higher than the other amphibolites. Its MgO content is extremely low (1.4 wt. percent), as is its CaO content. The Fe_2O_3/FeO ratio is higher than for any of the other rocks.

Trace Element Chemistry

Trace elements Rb and Sr have unsystematic variations, probably caused by alteration. The mafic volcanic rocks have much higher abundances of these elements than the high-Mg rocks. Yttrium, Zr and Nb abundances are about the same for both rock types, although a few from each type have exceptionally high abundances. The metasediments have significantly higher Zr and Nb abundances than the mafic and ultramafic rocks and the garnet amphibolite has the highest values of all.

In the mafic and ultramafic rocks the transition metals V and Cr show a large variation with Mg content, whereas Co shows only limited variation (Fig. 4a-c). The V content in these rocks decreases with increasing Mg num-

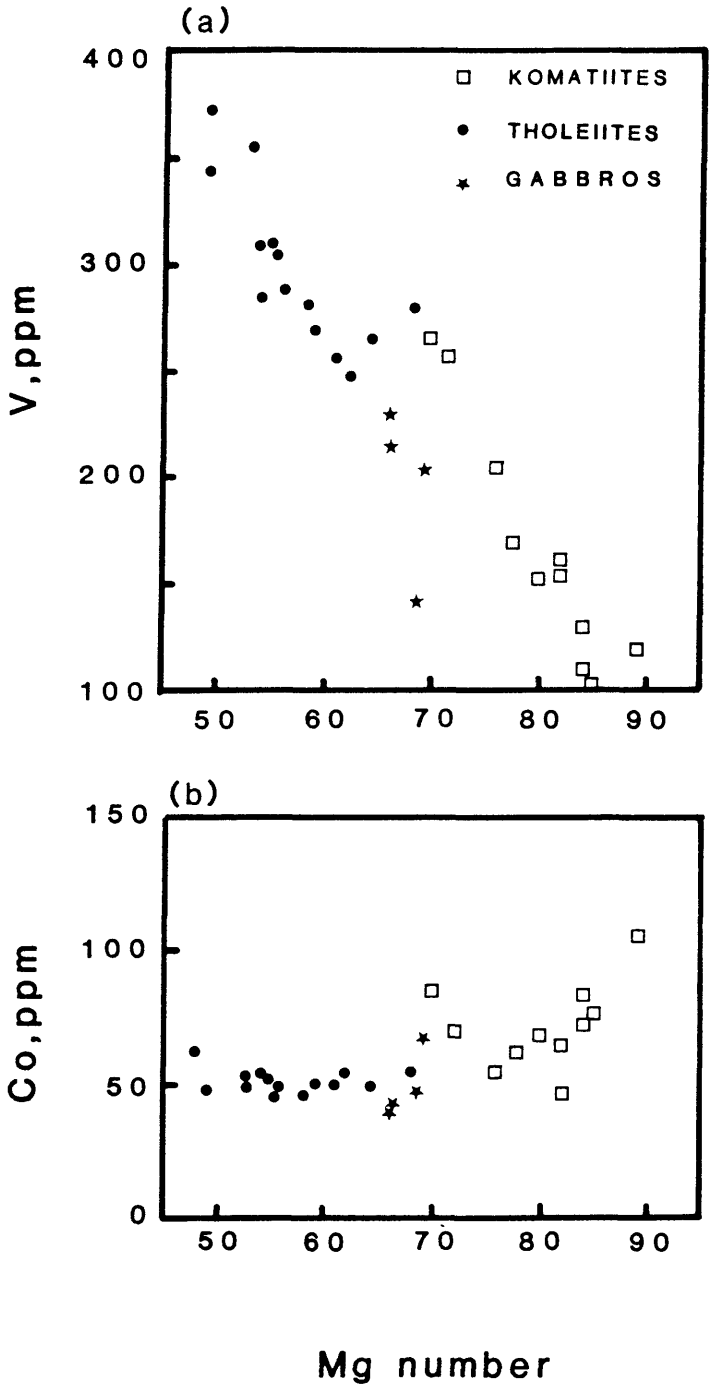

Figure 4.--Variation diagrams showing transition metals versus Mg number for rocks of igneous origin from the Elmer's Rock Greenstone Belt;(a) vanadium, (b) cobalt

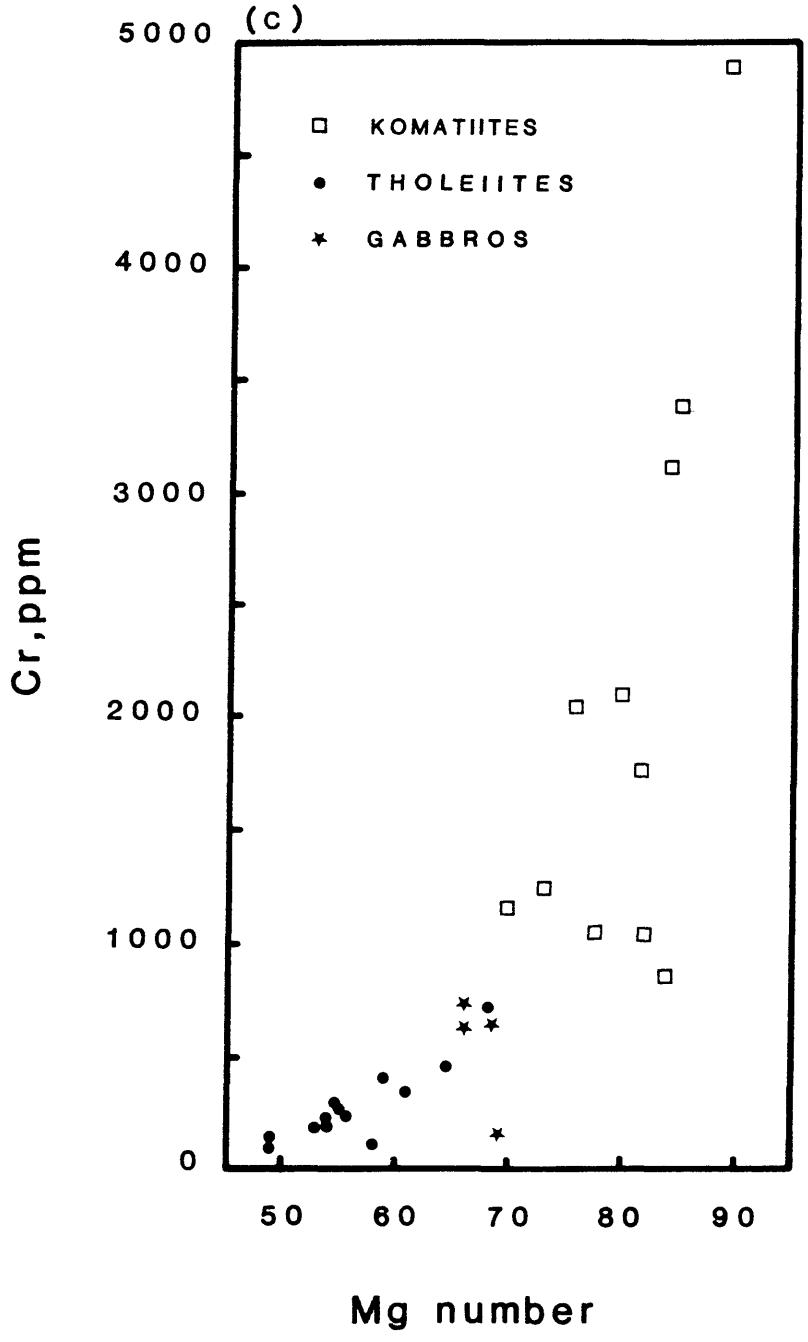

Figure 4.--(con't) (c)chromium.

ber. The decrease of V in the fine-grained mafic amphibolites is somewhat sharp but has a greater spread at higher Mg numbers. The range of V in these rocks is higher than in the other rock types; between 240 and 375 ppm. The ultramafic amphibolites show a sharp to moderate decrease in V as Mg number increases with a spread at higher Mg numbers. The V contents in the ultramafic amphibolites vary from 100 to 270 ppm. The coarse-grained amphibolite shows a dramatic decrease in V as Mg number increases. The range of V is from 140 to 230 ppm. This trend is different than the other two rock types.

The amount of Co in the fine-grained mafic amphibolites shows very little change as Mg number increases. All have approximately 50 ppm Co. The ultramafic amphibolites show no consistent variation of Co with Mg number. The range of Co in these rocks is from 40 to 70 ppm.

The fine-grained mafic amphibolites show a strong positive correlation between Cr content and Mg number. These rocks have a lower Cr content than the ultramafic amphibolites; less than 800 ppm. The ultramafic amphibolites have a steep positive correlation between Cr and Mg number with a Cr range between 800 and 5000 ppm. At the lower end of Cr contents there is less variation of Cr with Mg number. There is a break in slope between the ultramafic

and mafic amphibolite compositions. All but one of the coarse-grained amphibolites fit into the fine-grained amphibolite trend. If this sample is taken into account, the coarse-grained amphibolites show a somewhat negative correlation between Cr and Mg number.

Rare Earth Elements

The natural abundances of all elements vary in relation to one another and cause irregularities in their patterns when abundance is plotted versus atomic number. This is known as the Oddo-Harkens effect. The analyzed REE values were normalized to chondrite values (Hanson, 1980; Table IC.) for the purpose of interpretation, to eliminate irregularities in the patterns. All high-Mg rocks are light rare earth element (LREE) enriched (Fig.5). The $(Ce/Nd)_N$ for the non-cumulate rocks, those without positive Eu anomalies, is around 1.4. Ce abundances range from 2 to 100 times chondrite (xCHON). Samples ER122 and ER113 also have heavy rare earth element (HREE) depletion. Ytterbium abundances are 1 to 10 xCHON. Samples ER112 and ER119 have positive Eu anomalies ($Eu/Eu*=1.98\pm.25$).

The fine-grained mafic amphibolites (Fig. 6) have patterns with abundances of all REE from 6 to 20 xCHON. The $(Ce/Nd)_N$ ratio of the mafic amphibolites (~1) is very

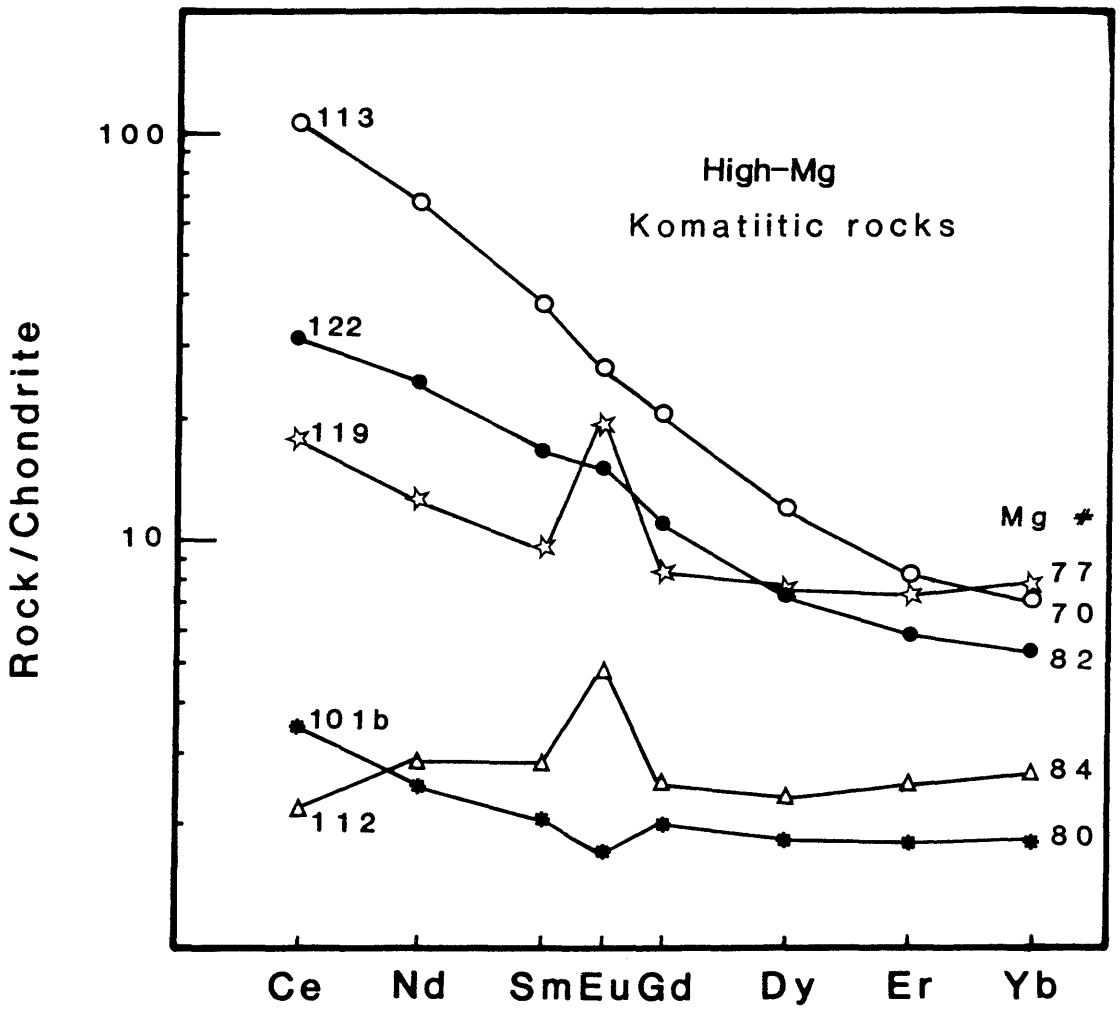

Figure 5.--Chondrite normalized REE patterns for high-Mg (komatiitic) rocks from the Elmer's Rock Greenstone Belt. Mg numbers are listed on the right of the diagram.

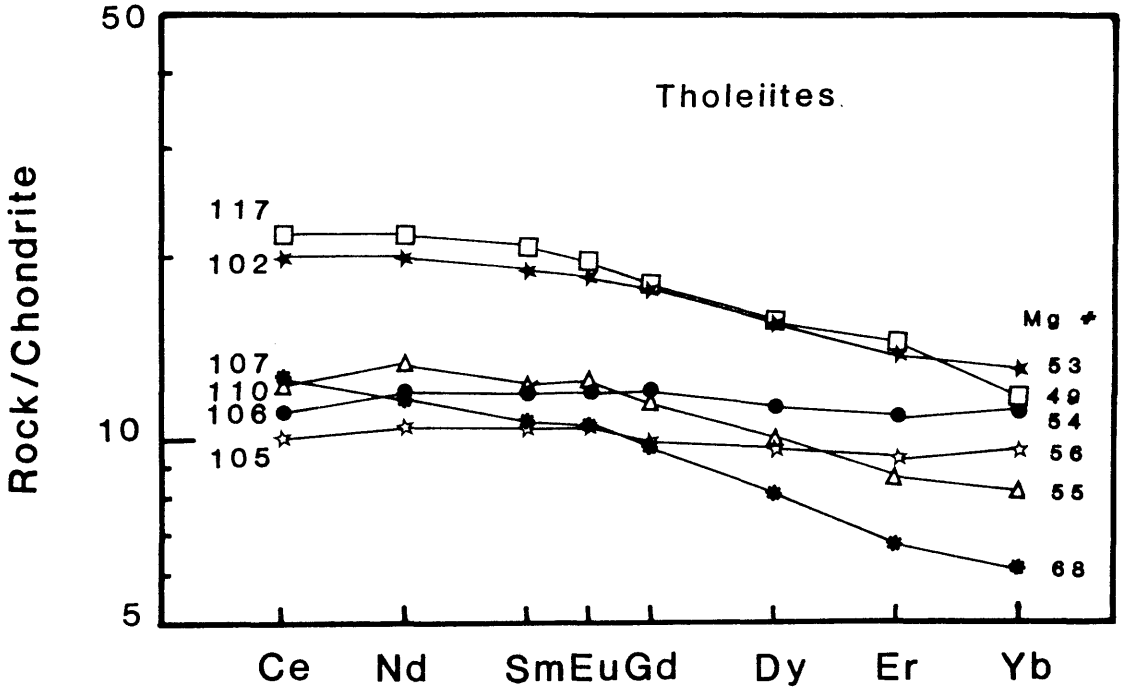

Figure 6.--Chondrite normalized REE patterns for fine-grained amphibolites (tholeiites) from the Elmer's Rock Greenstone Belt. Mg numbers are listed on the right of the diagram.

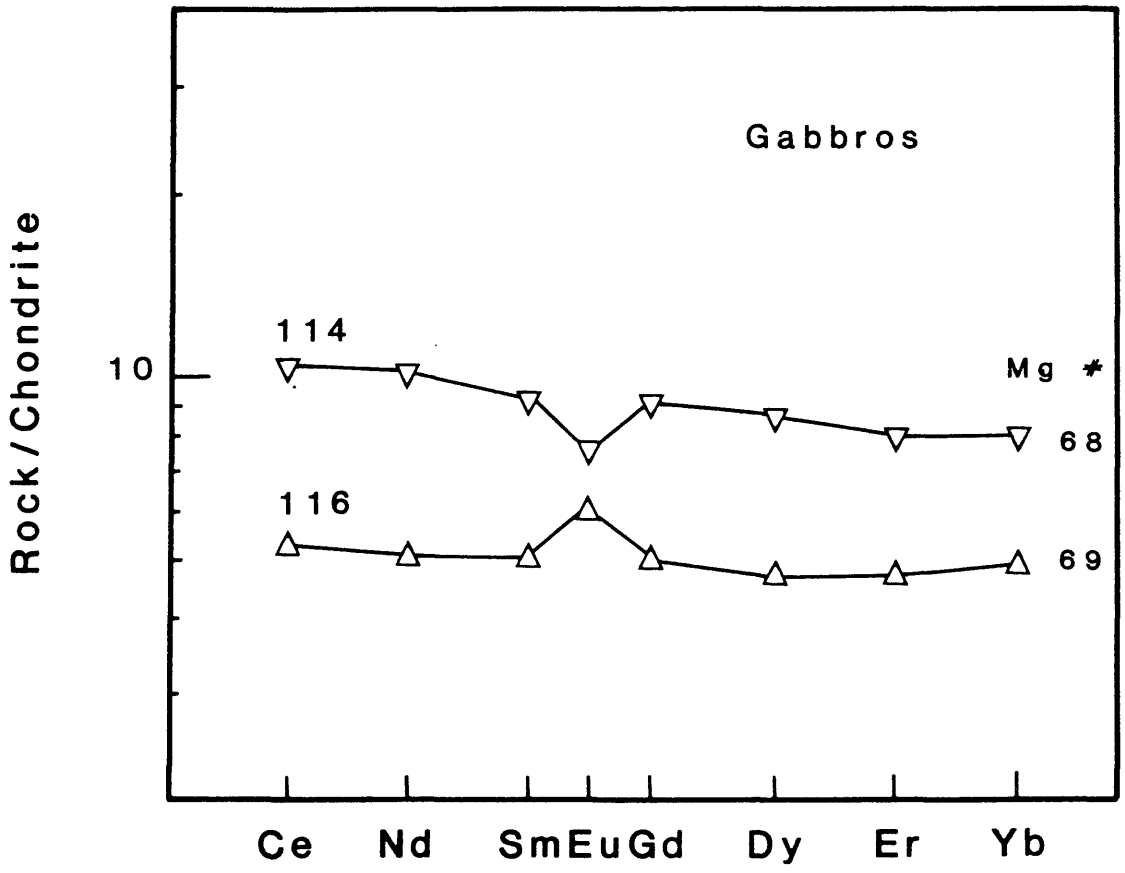

Figure 7.--Chondrite normalized REE patterns for coarse-grained amphibolites (gabbros) from the Elmer's Rock Greenstone Belt. Mg numbers are listed on the right of the diagram.

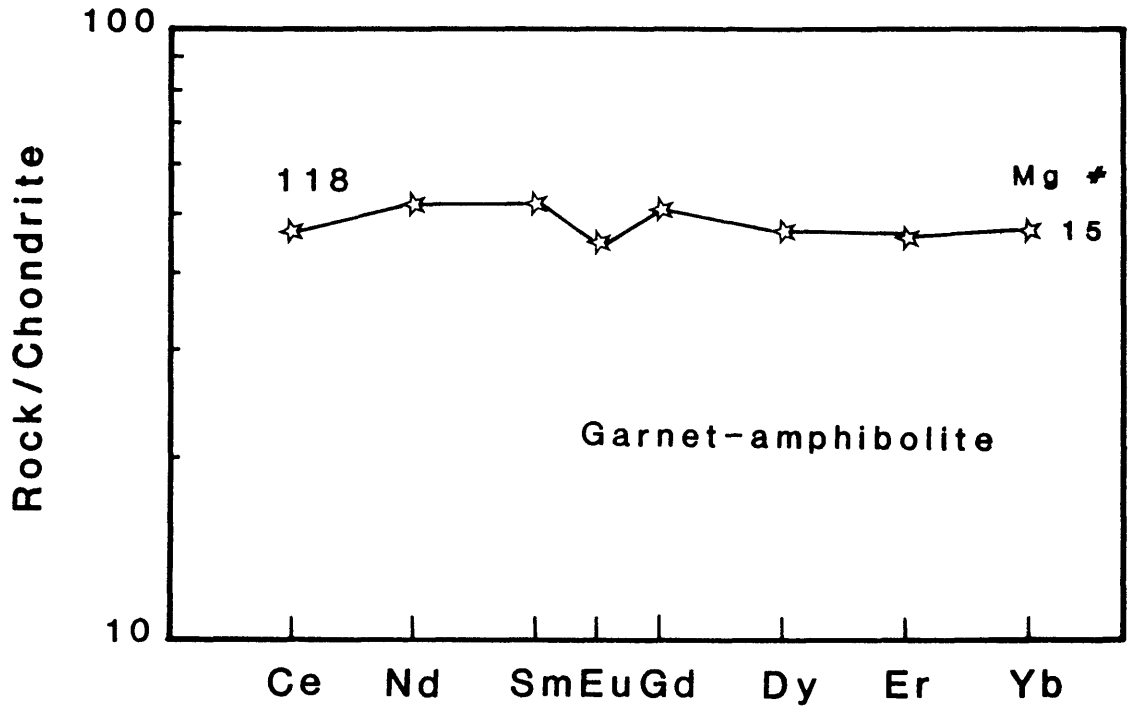

Figure 8.--Chondrite normalized REE patterns for a garnet amphibolite from the Elmer's Rock Greenstone Belt. Mg number is listed on the right of the diagram.

different from that of the ultramafic rocks. One of these amphibolites has a slightly LREE enriched, fractionated pattern. The others have flat to slightly depleted LREE and flat to depleted HREE. None show any significant Eu anomaly. Mg numbers show a slight decrease as total REE content increases.

The REE patterns for the coarse-grained mafic amphibolites are shown in Fig 7. They are relatively flat patterns with REE abundances between 5 and 10 xCHON and have complimentary Eu anomalies ($\pm$.2).

The garnet amphibolite REE pattern is shown in Fig. 8. It has a relatively flat pattern with a small negative Eu anomaly and a slight depletion of Ce. This pattern is enriched relative to the fine-grained amphibolites (50 xCHON) and has a Mg number of 15, which is significantly different from the other rocks.

The two metagreywacke samples (Fig. 9) are severely LREE enriched [$(Ce/Sm)_N$=16.9$\pm$.2] and somewhat depleted in HREE [$(Gd/Yb)_N$=2.14$\pm$.1] but $(Er/Yb)_N$=1 (Fig. 10). Both have small Eu anomalies.

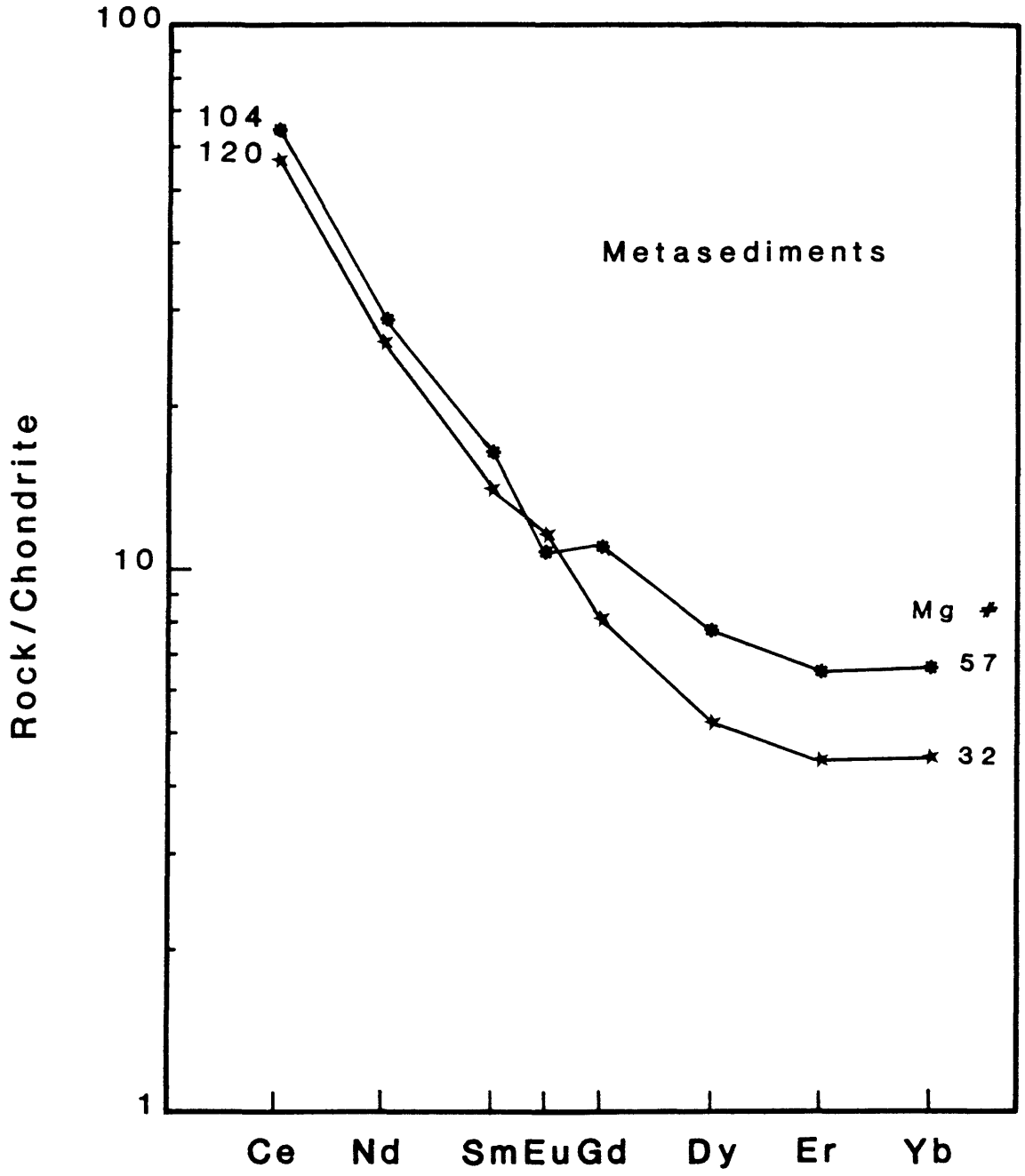

Figure 9.--Chondrite normalized REE patterns for metasedimentary rocks from Elmer's Rock Greenstone Belt. Mg numbers are listed on the right of the diagram.

CLASSIFICATION OF AMPHIBOLITES

The classification of rocks in Archean greenstone belts has been based on field, textural and chemical characteristics (Viljoen & Viljoen, 1969; Naldrett & Arth, 1976; Condie, 1976; Jensen, 1976; Arndt, 1977; Nesbit, et al, 1979). Since original igneous textures are often obliterated when mafic and ultramafic rocks are subjected to high grades of metamorphism, the classification of these rocks must be based primarily on the geochemical characteristics. The primary minerals and textures of the rocks in the ERGB have been eliminated by subsequent metamorphism to conditions of the amphibolite facies. Mafic and ultramafic rocks in Archean greenstone belts are generally tholeiitic and komatiitic. It is assumed, in our interpretation of the geochemical data, that the mafic and ultramafic rocks represent magmas at the time of their emplacement. It is possible that some of these rocks may represent cumulates, especially those with high MgO, as the chemical characteristics of some of these rocks suggest.

The first attempt at classifying the original rock type of the amphibolites from the ERGB was based on major elements. The classification scheme of Jensen (1976) was coupled with that of Arndt & Nesbitt (1982b) and Arndt

(1977). Figure 10 shows the composition of these rocks plotted on a Jensen cation diagram. Arndt & Nesbitt (1982b) consider ultramafic volcanics with greater than 18 percent MgO on an anhydrous basis to be komatiites and associated volcanics with between 18 and 9 percent MgO to be komatiitic basalts. The fine-grained amphibolites plot in the tholeiitic field on the Jensen cation diagram. One sample, ER107, falls into the border region between komatiitic and tholeiitic basalt. The coarse-grained amphibolites (ER114, ER116, ER-7, and ER-11) have a trend from tholeiitic compositions toward calc-alkaline compositions. Because of the coarse-grained nature of their texture and their occurrence as intrusive bodies (Snyder, 1984), they are considered to be gabbros. These classifications are supported by the use of a CaO-MgO-Al_2O_3 ternary diagram such as that of Condie, 1981 (Fig. 11).

Trace elements were used to further support the rock classifications. As Fig. 4a-c shows, there are distinct differences in the ratios of transition metals to Mg number for each rock type.

REE were also helpful in classifying the protoliths of these amphibolites. According to the above classification, samples ER101a, ER101b and ER-19 are ultramafic komatiites. Most komatiitic rocks described in the litera-

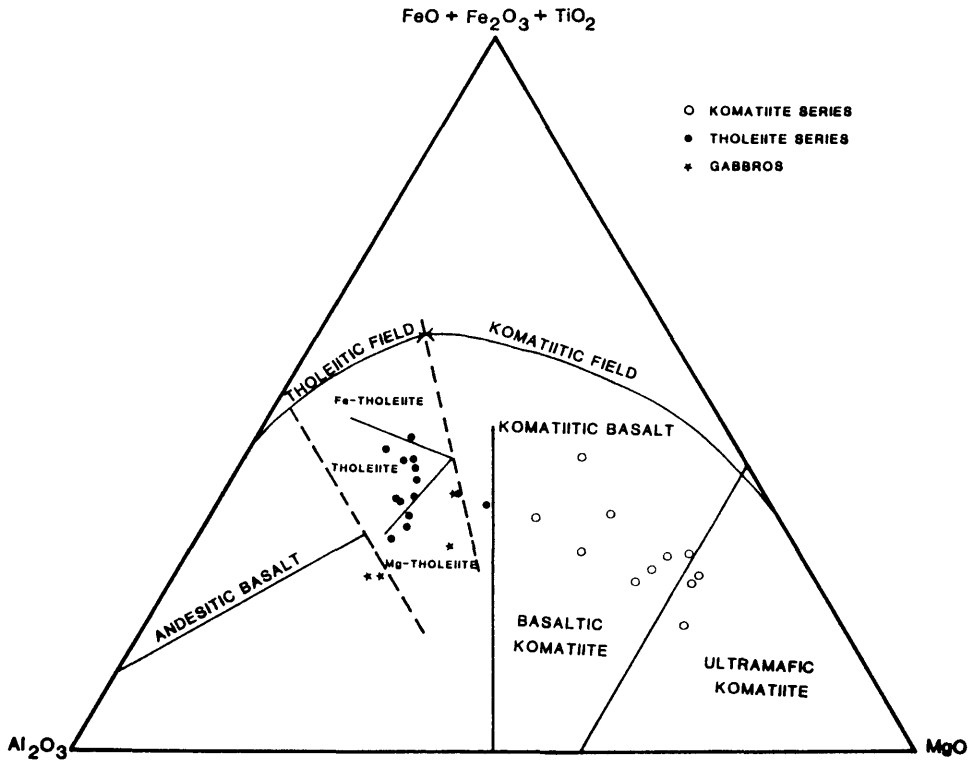

Figure 10.--Jensen cation plot for igneous rocks of the Elmer's Rock Greenstone Belt; used to discriminate between komatiite and tholeiite compositions (Jensen, 1976).

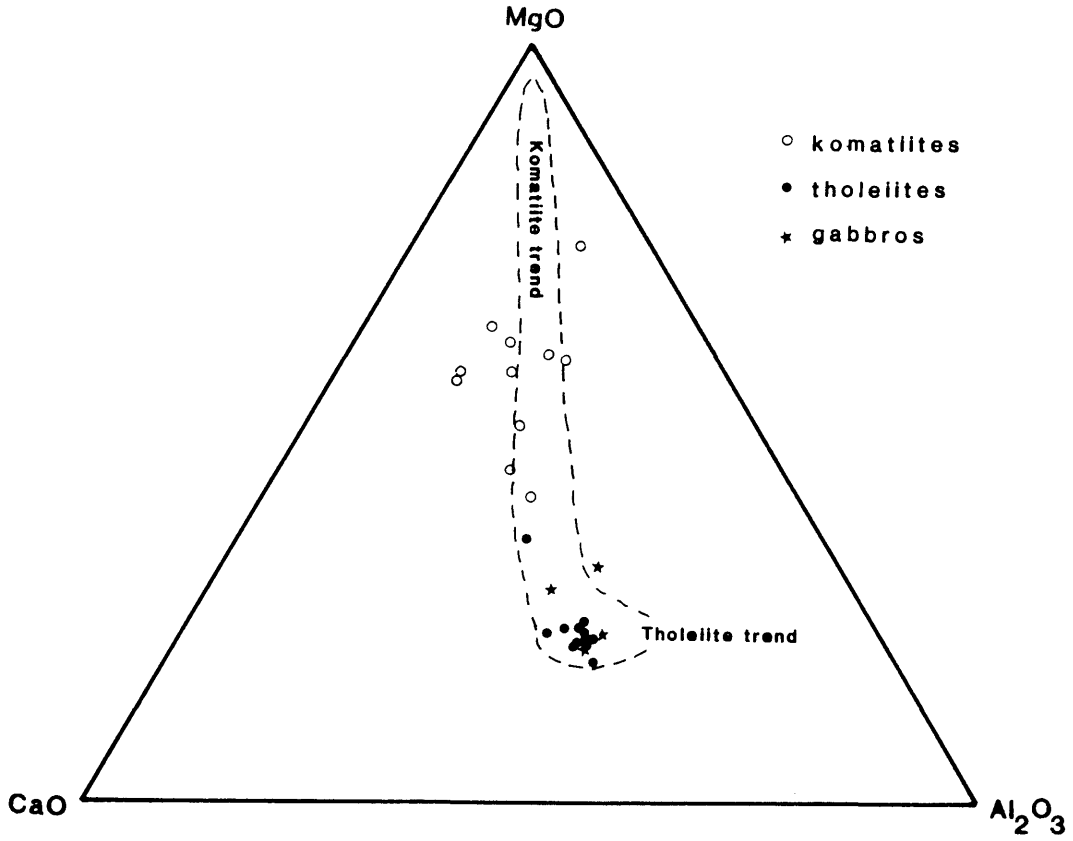

Figure 11.--CaO-MgO-Al_2O_3 diagram for the mafic and ultramafic rocks of the Elmer's Rock Greenstone Belt. These rocks form a continuous spectrum from the komatiitic trend through the tholeiitic trend (Condie, 1981).

ture have flat to LREE depleted patterns (Arndt & Nisbet, 1982a; Basaltic Volcanism Study Project, 1981). The REE pattern for ER101b (Fig. 5) is typical of that for rocks with komatiitic compositions in that the total abundance of REE is low (2-3 xCHON). It does, however, have slightly enriched LREE which is unusual, but not unheard of, in komatiitic rocks (Arndt & Nisbet, 1982a). Samples ER112, ER121 and ER-14 are classified as basaltic komatiites. The low abundance pattern of ER112 supports its komatiitic affinity, but the positive Eu anomaly suggests that it may be at least partially cumulate.

Samples classified as komatiitic basalts are ER113, ER119, ER122, ER-15 and ER-17. The REE pattern for ER119 is typical (Hanson, 1980) for that of a cumulate rock (Fig. 5). Samples ER113 and ER122 are unusual in that they have LREE enriched, sloping patterns with slight HREE depletion. Sample ER107 is intermediate in composition between komatiitic and tholeiitic basalt. Its transition metal contents are similar to those of the other tholeiites although they are very close to those of the komatiitic rocks. The REE pattern of this sample (Fig.6) is slightly LREE enriched and fractionated and has a higher Mg number than any of the tholeiites in the suite. Its present mineralogy is similar to the tholeiites. Based

upon this information ER107 has been classified as a Mg-tholeiite for the purpose of this study.

The tholeiitic rocks in this suite range in composition from Mg-tholeiite to Fe-tholeiite. They have flat REE patterns (Fig.6) similar to those of other Archean tholeiites (Basaltic Volcanism Study Project, 1981) with the exception of being slightly HREE depleted.

The geochemical characteristics of the tholeiitic and komatiitic rocks of the ERGB are similar to those of other greenstone belts. The exception to this is the highly fractionated patterns of the komatiitic basalts. The unique characteristic of these rocks will be emphasized in the discussion of the petrogenesis of these rocks.

TABLE 3.

Comparison of Greenstone belts.

Komatiites:	(1)	(2)	(3)	(4)
SiO_2 %	44-50	46-52	44-46	44-51
MgO	24-39	12-20	29-33	8-34
TiO_2	.2-.5	.5-.9	.24-.3	.2-.8
Al_2O_3	2-5	10-14	5-7	3-15
CaO	3.5-10	8-11	5-6	4-12
Na,K,P	tr	tr	tr	tr
Cr ppm	3000-6000	1000-3000	2800-3200	200-6000
Ni	1100-2700	200-800	1500-1700	50-2000
Zr	10-30	22-30	13-17	150-1600
Y	3-10	12-30	6-7	9-40
Nb	<1-2.5	.1-3	.2-1.3	---
V	70-125	175-230	114-124	20-400
REE		LREE	LREE	
	flat	dpl	dpl & enr	flat
(x CHON)	1	0-5	0-10	1-10
Tholeiites:	(1)	(2)	(3)	(4)
SiO_2 %	48-52	50-52	49-53	50-51
MgO	6-13	8-13	6-13	6-7
TiO_2	.5-1.5	.4-.9	.5-1.7	2
Al_2O_3	6-16	8-14	10-14	13
CaO	8-12	8-13	---	9
Na,K,P	tr-4	tr-4	tr	tr-3
Cr ppm	---	200-2000	120-1400	20-600
Ni	---	75-600	55-310	25-500
Zr	---	20-70	85-105	4-10
Y	---	11-25	14-30	10-20
Nb	---	160-300	215-300	200-1600
REE		LREE		LREE
	---	flat-enr	---	enr
(x CHON)		1-10		10-100

(1) Barberton; pC (Viljoen & Viljoen, 1969a&b; Smith & Erlank, 1982); (2) Abitibi/Munro Twnsp; pC (Arndt & Nisbet, 1982; Ludden & Gelinas; 1982); (3) Yilgarn, W. Australia; pC (Binns, et al, 1982; Anhaeusser, 1969, Nesbitt & Sun, 1976); (4) Finland; pC (Jahn, et al, 1981).

TABLE 3. (con't)

Comparison of greenstone belts.

Komatiites:		(5)	(6)	(7)	(8)
SiO_2	%	45-48	46-52	44-47	46-53
MgO		14-21	12-16	15-21	14-31
TiO_2		.75-1.5	.5-2.5	.4-.7	.18-1.8
Al_2O_3		6-12	10-12	10-13	4-11
CaO		8-12	7-14	9-11	3-12
Na,K,P		tr-1	tr-4	tr-1.5	tr
Cr	ppm	1300-3500	400-100	---	850-5000
Ni		700-1150	130-400	---	---
Zr		30-80	85-300	---	8-180
Y		13-20	---	---	2-25
Nb		<1-8	---	---	0-31
V		200-300	---	---	100-360
REE		MREE enr	LREE enr	LREE dpl	LREE enr
(x CHON)		10-100	1-100	1-10	1-100

Tholeiites:		(5)	(6)	(7)	(8)
SiO_2	%	50-56	50-56	47-53	50-53
MgO		6-9	9-11	5-11	6-11
TiO_2		.6-1.5	.75-1.25	.7-1.9	.5-2
Al_2O_3		13-17	11-16	13-14	12-16
CaO		7-14	7.5-12	8-13	10-12
Na,K,P		tr-3	tr-3	tr-3	tr-3
Cr	pp	100-1000	110-325	---	35-715
Ni		80-200	40-400	---	---
Zr		50-100	50-140	---	25-100
Y		13-30	---	---	9-150
Nb		<2-14	---	---	0-5
V		200-315	---	---	250-360
REE		flat	LREE enr & dpl	flat	HREE dpl & flat
(x CHON)		5-10	1-10	10-20	1-10

(5) Kolar Schist Belt, India; pC (Rajamani, et al, 1985); (6) Klamath Mtns.; P-Tr(Ernst, 1987); (7) Gorgona Islands, Columbia; T(Echeverria, 1982; Aitken & Echeverria, 1984); (8) Elmer's Rock belt; pC (this study).

PETROGENESIS

The source type and conditions of melting and differentiation for the rocks described above will be evaluated in this section. The most effective evaluation of the petrogenesis of a rock is based on a total analysis of both major and trace elements. Our interpretation of these rocks was based on the approach used by Langmiur & Hanson, 1981 and Hanson & Langmuir, 1980 for major elements and, Hanson, 1980 for trace elements. Sixteen samples which have the most complete analyses, including REE, were used in our evaluation. Other samples are referred to when necessary.

There is a broad spectrum of processes which form igneous rocks. We have evaluated the ERGB rocks using the simplest models possible: partial melting and fractional crystallization (Hanson, 1980). The equations which represent these processes are:

$$\frac{C_L}{C_o} = \frac{1}{(D(1-F)+F)} \qquad (1)$$

for batch melting (Schilling, 1966) and

$$\frac{C_L}{C_o} = F^{(D-1)} \qquad (2)$$

for fractional crystallization (Neumann, 1954). In these

equations C_o represents the initial concentration of the element in the system, C_L is the concentration of the element in the melt, F is the amount of melt or residual liquid and D_o is the bulk solid-melt distribution coeffecient at the time of removal of the melt (Hanson, 1980). The bulk distribution coefficient is defined by:

$$D_o = \Sigma X_i K_d = C_s/C_L \qquad (3)$$

where X_i is the fraction of each mineral in the solid residue, Kd is the single element distribution coefficient and C_s is the concentration of the element in the solid residual phases (Hanson, 1980). For an incompatible element, D_o approaches zero and for both processes.

$$F \sim C_o/C_L \qquad (4)$$

Incompatible trace elements in basic igneous rocks, such as LREE and Zr, are not fractionated from each other by melting or fractional crystallization.

In order to make a quantitative evaluation of the nature of the processes which formed a rock, the most precise and accurate data available should be used. For the ERGB rocks, the REE fit this criterion since they were analyzed by the isotope dilution method.

Since Ce has the lowest Kd for most minerals (Arth, 1976), it is chosen as the most incompatible element to

be used for these calculations. Setting $D^o \sim 0$, the amount of melting or crystallization required to produce these rocks was calculated using equation (4). It is not important what the value for D^o actually is, as long as it is small (<0.1).

Once the amount of melting or fraction of residual liquid was calculated, the D_o's for other trace elements were calculated using equations (1) or (2). Mass balance calculations of major elements were done to obtain the total composition of the resulting residual phases using the equation

$$C_s = \frac{C_o - (F)\ C_L}{1 - F} \qquad (5).$$

Using the proportions of the phases calculated by mass balance and Kd's for individual minerals, bulk distribution coefficients for the residual assemblage were calculated. The D_o's calculated for these two methods were then compared to each other to evaluate which model best fit the given rocks.

A number of Kd's have been determined experimentally for many igneous minerals in various rock types (eg. Schnetzler & Philpotts, 1970; Arth, 1976). The best possible choice of Kd's for use in quantitative interpretations would be those determined from the original

minerals which compose the rock. Unfortunately, this is not possible for the ERGB rocks due to total recrystallization during metamorphism. Hence, we have used the next best choice by comparing the chemical properties of the ERGB rocks with those reported for rocks from which the Kd's have been determined and using those Kd's.

For all cases in which we assumed that the rocks represented liquid compositions (ie. those without significant Eu anomalies) a partial melting model best fit the data. A source of pyrolite composition (Ringwood, 1975) was used for all of the partial melting model calculations.

Hanson & Langmuir, 1978, used a trace element approach, such as that described above, to model mantle-melt systems with the major elements MgO and FeO. Using the olivine saturation surface of Roeder & Emslie (1970), they calculated melt and residue fields, using a FeO-MgO exchange reaction Kd of 0.3 between olivine and basaltic melts for batch melting of a pyrolite mantle source. Temperatures were calculated at one atmosphere. Higher temperatures would shift the melt field to the left by about 5°C per kb (Langmuir & Hanson, 1980). Figure 12 shows the melt and residue fields for these calculations as well as liquid lines of descent for the fractionation

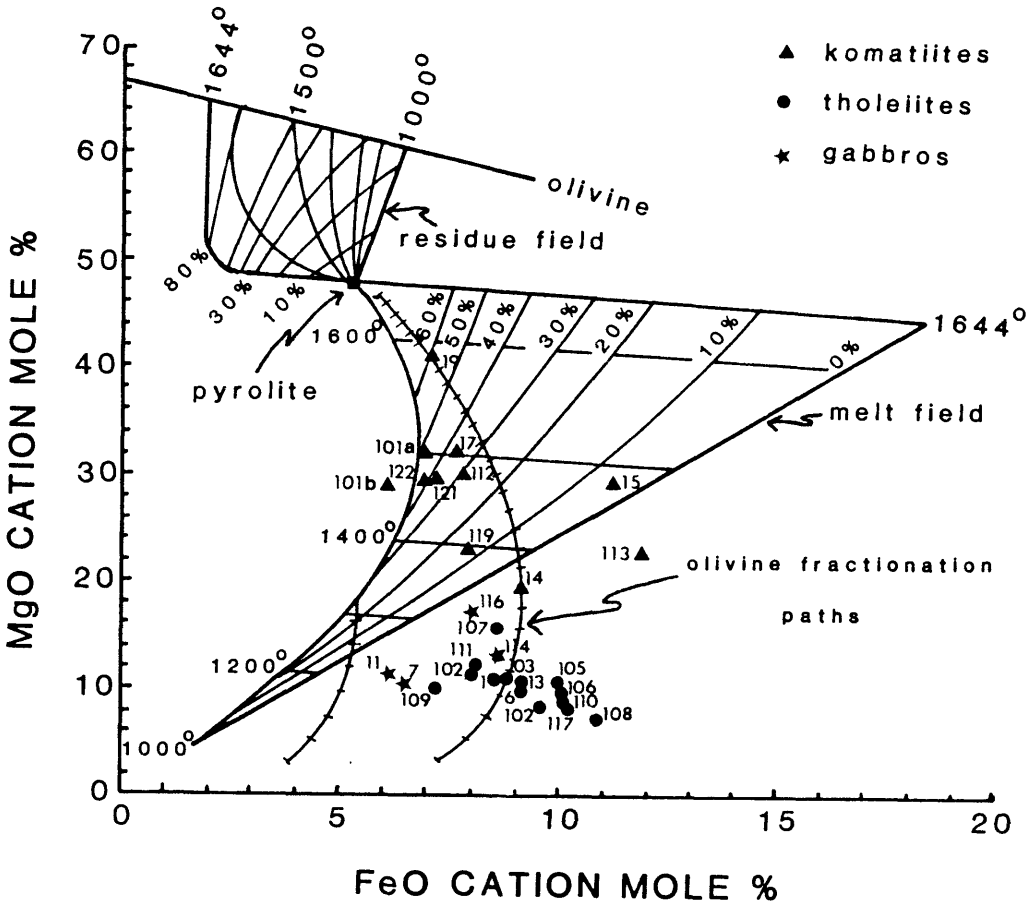

Figure 12.--Olivine saturation diagram for Elmer's Rock Greenstone Belt rocks (after Hanson & Langmuir, 1978). The `sail' represents the field of liquid compositions derived by melting a pyrolite source. Horizontal lines are isotherms, diagonal lines represent degrees of melting and curves with tick marks are liquid lines of descent for olivine (each tick represents 5% fractionation from the last tick mark). Komatiitic rocks plot mainly in the melt field while tholeiitic rocks fall below the field.

of olivine alone. Mantle derived melts fall within or below the melt field, depending upon the nature and extents of fractionation and temperature and degree of melting. When pyroxene or plagioclase crystallize along with olivine, the resulting melt becomes more enriched in FeO than if olivine were crystallizing alone.

The majority of the ultramafic rocks plot in the primary melt field of the olivine saturation diagram Fig. 12). The most primitive rock, ER101b, plots just to the left of the melt field in the region known as the "forbidden zone" (Hanson & Langmuir, 1978). Rocks which plot in this zone would exceed the maximum amount of partial melting allowable under these conditions. This diagram represents conditions of melting of a pyrolite source at 1 atm., which is an unlikely pressure for deep mantle rocks. If the melt field is adjusted for higher pressures (Hanson & Langmuir, 1978) it would be shifted to the left enough to include ER101b in the melt field. A shift in the position of this field can also be a function of Kd's or starting composition (Langmuir & Hanson, 1980). ER113 lies below the melt field suggesting fractionation of olivine and possibly other minerals during its formation.

All of the tholeiites fall well below the primary melt field on the olivine saturation diagram (Fig. 12).

This implies fractionation of olivine from a primary mantle-derived melt. The trend of the tholeiites to spread out along the FeO axis at approximately constant MgO may be explained by the fractionation of pyroxene and/or plagioclase along with olivine. ER107 is closer to the melt field than the other tholeiites and does not fall into this trend.

The regions in which these two rock types plot on the olivine saturation diagram suggests they were derived by sources with similar major element composition but by somewhat different mechanisms. The differences in Mg number and LREE fractionation are significant. The differences between the komatiitic and tholeiitic rocks are best represented when $(Ce/Nd)_N$ is plotted against wt. percent MgO (Fig. 13). This diagram also shows that ER107 lies between the two fields and appears to be a mixture of komatiitic and tholeiitic liquids. The gabbroic rocks do not fit into either field.

Komatiitic rocks

The ultramafic rocks of the ERGB have major element compositions of komatiitic affinity. The trace elements of these rocks, particularly the REE are unlike most Archean komatiitic magmas. The regularity of the REE pat-

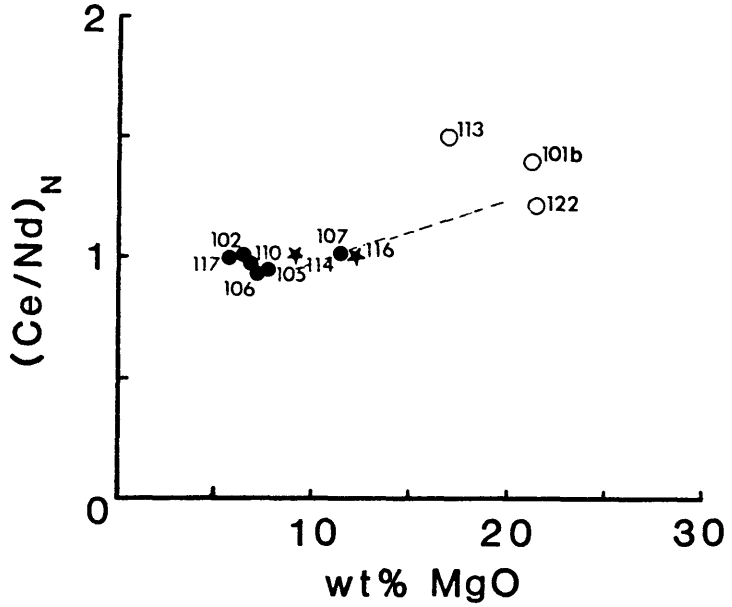

Figure 13.--$(Ce/Nd)_N$ versus wt.% MgO diagram for komatiites and tholeiites from the Elmer's Rock Greenstone Belt which best distinguishes features between these rock types. Sample ER107 falls between the two fields and may represent mixing of the two melts.

terns suggests that they represent original igneous patterns. Two of the five ultramafic samples which were analyzed for REE (Fig. 5) two, ER112 and ER119, have significant positive Eu anomalies which suggest accumulation of plagioclase. They will be discussed later in this section. Three rocks, ER101b, ER113 and ER122, have similar LREE enrichment ($(Ce/Nd)_N$=1.3-1.5). Of these, ER113 and ER122 have strongly fractionated chondrite normalized patterns with LREE abundances greater than most reported Archean ultramafic lavas (Table 3). Sun & Nesbitt, 1978a, observed LREE enriched patterns in spinifex-textured basalts of the Negri volcanics from Australia as did Rajamani, et al, 1984, from amphibolites in the Kolar Schist Belt of India. None of these rocks is as enriched as ER113 (Ce~100xCHON). Volcanic rocks of Permo-Triassic age with komatiitic affinities and similar trace elements have recently been reported by Ernst, 1987 and may have significance for the ERGB rocks. Sample ER101b has lower abundances, comparable with other Archean komatiites, with flat HREE and a slight negative Eu anomaly. It is likely that the Eu anomaly in this rock is due to alteration effects and not plagioclase accumulation since plagioclase is not a residual mineral after the extraction of high MgO melts (Green, et al, 1975; Green & Ringwood,

1967; Arndt, 1976) nor is early plagioclase saturation in a peridotitic komatiite likely (Green, et al, 1975; Arndt, Arndt, 1976).

Since the $(Ce/Nd)_N$ ratios of these rocks are so similar one might conclude that they were derived from the same LREE enriched source. It is also possible that the magma was contaminated by crustal material on its ascent to the surface (Arndt & Jenner, 1986; Barley, 1986; Compston, et al, 1986; Groves, et al , 1986; Sparks, 1986; Huppert & Sparks, 1985a, 1985b). If this were the case, differences in the fractionation of trace elements, depending upon the amount of contamination, would be expected. This is not observed in the ERGB rocks. Assimilation of crustal material may also change the bulk composition of the melt (Barley, 1986) although Huppert & Sparks, 1985a, have shown that up to 30 percent contamination of komatiite liquid by crustal material can occur without significant change in some rocks. The consistent compositions of these rocks, particularly the constant $(Ce/Nd)_N$ ratio, which is not a function of the abundance of the LREE, suggest that crustal contamination probably did not occur on any significant level but it cannot be totally ruled out with the evidence at hand. Contamination may however, explain the slightly higher

silica content of the komatiitic rocks. Isotope studies may help determine if contamination was involved in the evolution of these rocks (Barley, 1986; Sparks, 1986).

It is probable that the source may have been enriched sometime prior to the melting which produced magmas parental to these rocks and that the LREE enrichment of these rocks represents an original source characteristic. Sun & Nesbitt, 1978a, argued that the LREE patterns of peridotitic liquids will not be much different than their source and that HREE patterns may be affected by residual garnet or clinopyroxene. Our interpretations are based on this premise.

Mantle metasomatism by CO_2-rich fluids can enrich or deplete a source in incompatible elements such as REE, Ti, Zr, Nb, and Y (Schneider & Eggler, 1986; Wass et al, 1980; Wendlant & Harrison, 1979; Wyllie, 1979; Lloyd & Bailey, 1975). If the fluids pass through the source and extract these elements, the source becomes depleted in these elements. If, however, fluids rich in IE elements penetrate and crystallize in the source, an enrichment of these elements occurs in the source. The REE usually do not exist as ionic species, rather they precipitate in minerals such as carbonate and phlogopite (Spera, 1981). Most research on mantle metasomatism has been used to

explain the generation of alkaline magmas from peridotite beneath continental crust (Schneider & Eggler, 1986; Wass & Rodgers, 1980; Wyllie, 1979; Lloyd & Bailey, 1975). The REE patterns of the komatiitic basalts are similar to those of alkali basalts but their major element composition is quite different (Basaltic Volcanism Study Project, 1981; Carmicheal, Turner and Verhoogen, 1974). Because the major elements are decoupled from the trace elements for the case of the komatiitic rocks, an introduction and equilibration of IE-enriched fluids into the original melt from another region may be a better explanation for the trace element enrichment in these rocks than a total metasomatism of the source. In this case metasomatism would have affected only the trace elements but not the major element composition of the source.

Another possible explanation for the IE enrichment of these rocks is the mixing of a strongly enriched melt of unknown origin with a melt derived from the mantle. The enriched melt would have to have had a similar major element composition as that of the mantle melt. In a modern tectonic setting, melting of eclogite from a subducting slab at great depth could produce such a melt (Apted, 1981; Ringwood, 1975). Whether this type of mechanism is valid for the Archean is uncertain. A choice as

to which of the above explanations is best for these rocks can not be based on the evidence we now have.

A petrogenetic relationship between the ultramafic komatiite and the komatiitic basalts based on fractional crystallization is unlikely. Over 97% fractional crystallization of a liquid the composition of ER101b would be required to produce that of ER122 (Table IIIA). This large amount of fractional crystallization is improbable (Hanson, 1980) under most conditions. ER122 and ER113 can be related by 70% fractional crystallization of ER122 to produce ER113, leaving a residue of plagioclase and hypersthene. This would however, require extremely large mineral-melt Kd's for these minerals (see Appendix III). Distribution coefficients of this size have been reported (Green & Pearson, 1985; Fujimaki, et al, 1984; Schnetzler & Philpotts, 1970) but may not be appropriate to this rock type. The process which produced the higher silica content of these rocks may have influenced the partition coefficients of the major and trace elements in the minerals (Green & Pearson, 1985; Ford, et al, 1983; Kushiro, 1975). Unfortunately the primary mineralogy of these rocks has been obliterated and the Kd's for the original minerals can not be determined.

ER122 and ER113 can also be related by very small

degrees of partial melting of the same LREE enriched source. If these rocks represent products of partial melting then ER113 would represent 1% melting and ER122 would represent 4% melting, leaving almost identical residues composed of up to 20% garnet with plagioclase and pyroxenes. Evaluation of the komatiitic basalts separate from ER101b can not distinguish which model best explains the formation of these rocks.

ER101b and ER122 have almost identical major element compositions but have compositions which differ by factors of between 3 and 30. Based on the REE data, it is possible to relate ER101b and ER122 by different degrees of partial melting of a LREE enriched chondritic garnetiferous source. The major element chemistry and normative mineralogy of these two rocks are very similar. They also plot along the same isotherm on the olivine saturation diagram (Fig. 12). The decoupling of major and trace elements in these two rocks can be explained by pseudo-eutectic melting along the boundary where garnet is not a stable phase of the residue. This accounts for the HREE fractionation in the rock produced by the lowest degree of melting (10%) and for the unfractionated HREE in the more extensively melted (40%) rock. Eutectic melting would hold the major element composition of the

melt roughly constant while greater percentages of melting would affect the trace element compositions. The Mg number of ER101b (84) is slightly larger than that of ER122 (81) which supports some amount of fractionation.

If a partial melting relationship is accepted for the formation of ER101b and ER122 then the favored explanation for the production of ER113 from the same source is that of 70% fractional crystallization of a liquid with the composition of ER122. This model is supported by the more fractionated REE pattern and enrichment of other trace elements in ER113. The Mg number of ER113 (70) has evolved slightly from that of a melt in direct equilibrium with the mantle and is lower than the other ultramafic rocks.

The content of trace elements other than REE, such as Ti, Zr, Nb, and V are greater in ER122 than ER101b. The incompatible behavior of these elements during the melting process contributes to the depletion of later melts. Chromium acts as a compatible element (Fig. 4c) in these two rocks and cannot be explained by partial melting alone. Therefore, a phase such as Cr-spinel was probably present as a solid phase during early melting of the source (ER122) and was incorporated into the magma at higher degrees of melting (ER101b). The enrichment of Cr

in ER113 relative to ER122 can be explained by fractional crystallization. Cobalt also behaves as a compatible element in ER101b and ER122 but has fractionated away from a partial melting trend in ER113. The variation of Ti and Zr with MgO (Figs. 14 a&b) also supports the possible derivation of ER113 from fractional crystallization of the other komatiitic liquid.

Any relationship of ER113 and ER101b by different degrees of partial melting of a LREE enriched pyrolitic source is not supported by mass balance calculations of major and trace elements. Nor can all of these rocks be related by sequential melting of such a source, which places unreasonable constraints on trace element mineral-melt Kd's.

In summary, the most consistent explanation for the origin of these rocks is that ER101b and ER122 were produced by various degrees of partial melting, under close to eutectic conditions, of a LREE enriched garnetiferous pyrolite (garnet lherzolite) source and ER113 is fractionally crystallized from a liquid like ER122.

The other two ultramafic rocks (ER112 and ER119) which were analyzed for REE may be cumulates from either the komatiitic series or the tholeiitic series. The field locations of both of these samples occur in close proxim-

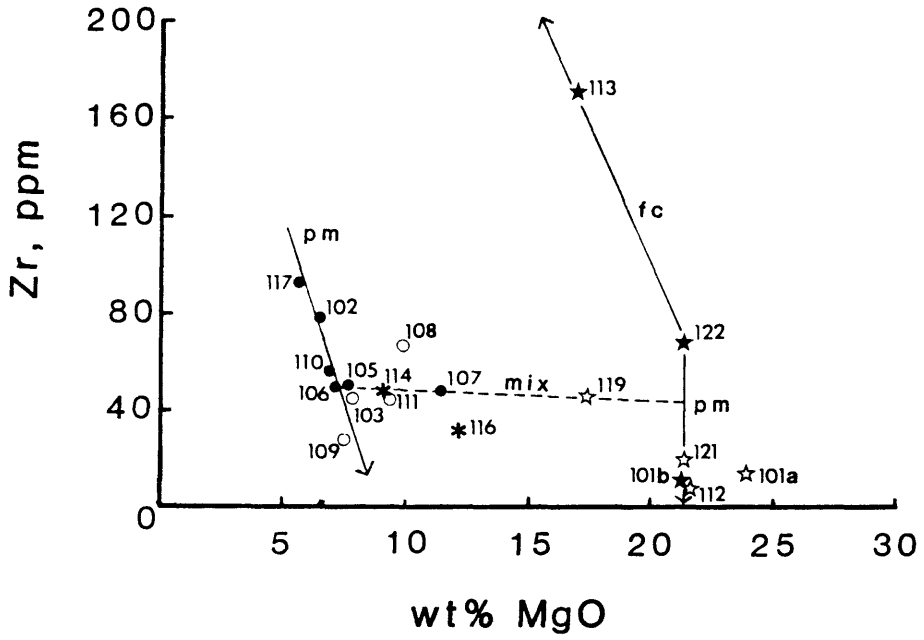

(a) Zr versus MgO

Figure 14.--Variation diagrams for selected samples from the Elmer's Rock Greenstone Belt. Partial melting (pm) and fractional crystallization (fc) trends (solid lines) are shown for each series. The filled symbols represent those samples which were used for interpretation. Sample ER107 falls between the two trends and may represent mixing (dashed line) of the melts. Other samples fall within these trends but were not included for clarity.

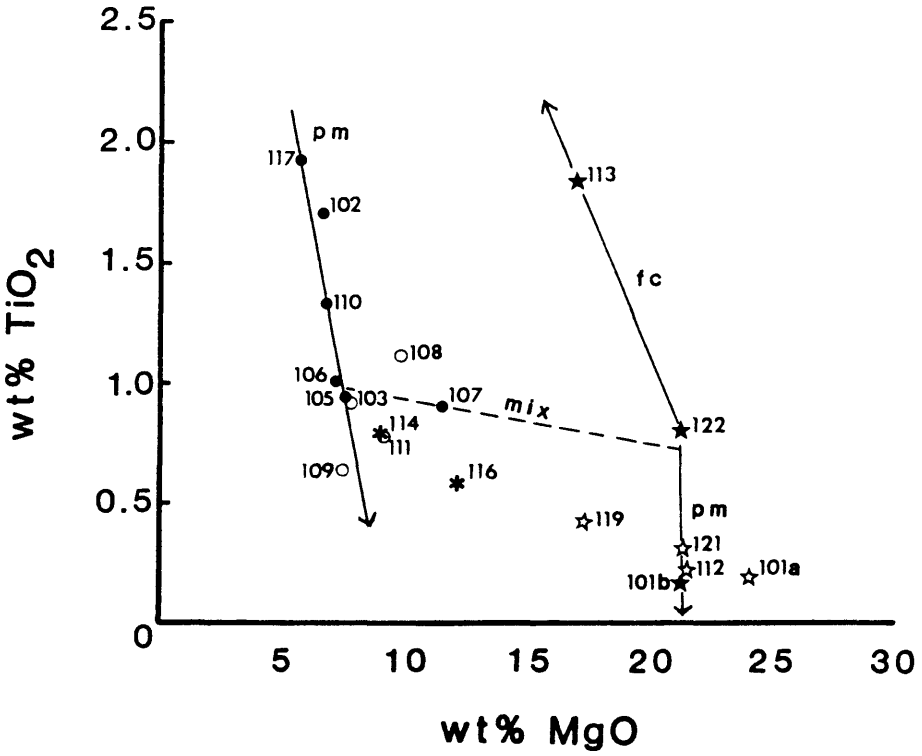

(b) TiO_2 versus MgO

Figure 14 (con't).

ity to other ultramafic schist units which may suggest that they are related to the komatiitic series. Mass balance calculations for ER119 (Table IIID) show that it could have been a mixture of plagioclase and pyroxene crystals plus a LREE enriched ferromagnesian liquid such as that of the komatiitic series, (Fig. 15a). It has a normative mineralogy of 10% olivine, 32% orthpyroxene, 28% clinopyroxene and 28% plagioclase. Thus, ER119 was probably a cumulate from the komatiitic series. ER112 may also be a cumulate from these rocks. Its normative mineralogy is 62% orthopyroxene, 18.5% clinopyroxene and 17% plagioclase. The calculated bulk distribution coefficient pattern of REE for this assemblage closely parallels the REE pattern of ER112 normalized to the liquid composition of ER122 (Fig 15b). This suggests that ER112 may be an adcumulate of the komatiitic series.

From the above discussion it can be seen that all of these ultramafic rocks are probably related to the same IE-enriched source by very different processes.

Tholeiitic rocks

The tholeiitic rocks are very different from the komatiitic rocks. Except for the high-Mg tholeiite (ER107), they all have flat to slightly depleted LREE

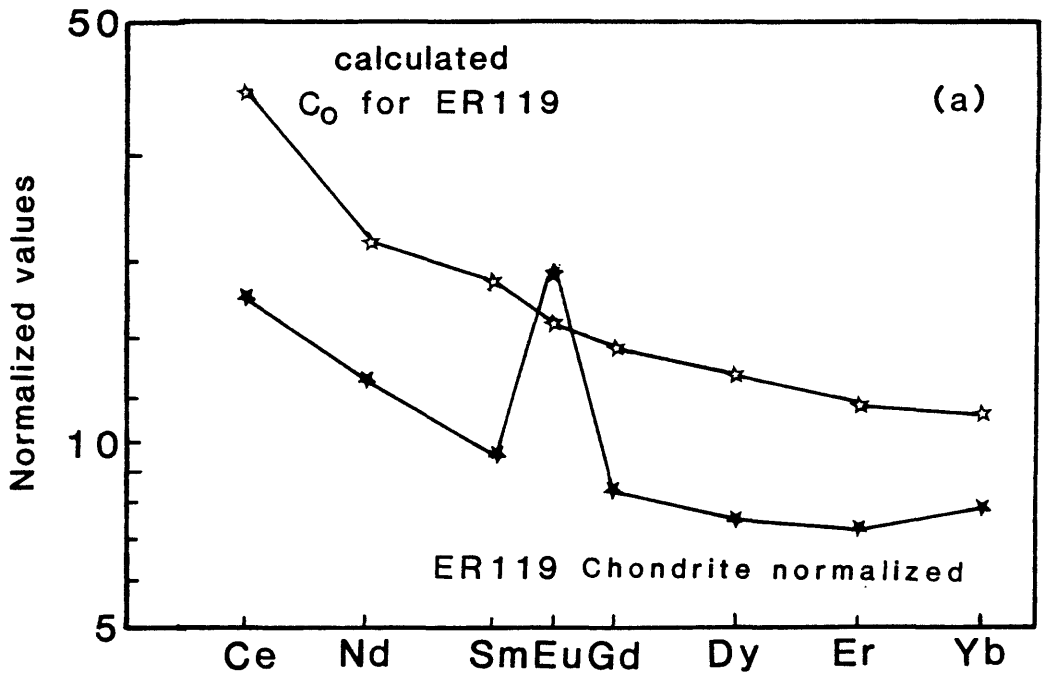

(a) ER119
(Kd's from GSFC271; Schnetzler & Philpotts, 1970)

Figure 15.--Calculated models for possible liquid and/or cumulate assemblages for samples ER112 and ER119.

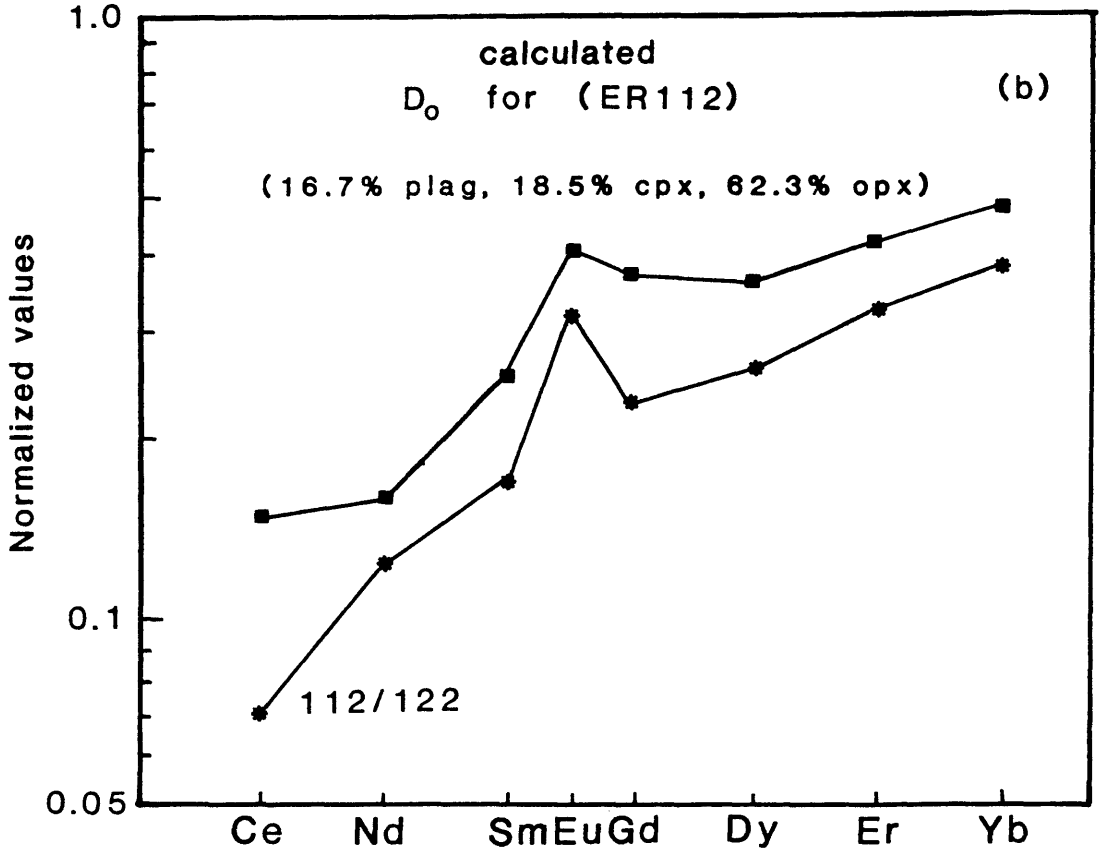

(b) ER112

Figure 15 (con't).

ratios and evolved Mg numbers (~50) suggesting that some fractionation from a primary mantle-derived melt must have occurred. Most have HREE depleted chondrite normalized patterns (Fig. 6). As REE content decreases in this series the amount of LREE depletion increases and HREE fractionation decreases. Both Zr and Ti decrease with decreasing REE content and the Mg number increases slightly with decreasing REE content.

Fractional crystallization alone can not produce these rocks but small degrees of partial melting of a slightly depleted chondritic garnetiferous source can explain the relationship between these rocks (Appendix III). If partial melting is the mechanism which controls the compositional variation in this suite, it must have occurred over a range of temperature and pressure conditions. The primary liquids frrom which ER117, ER102 and ER110 were derived , were in equilibrium with garnet while the primary liquids from which ER105 and ER106 were derived, do not show evidence for the involvement of garnet. It can be suggested that ER117 was the earliest of these liquids to form while still in equilibrium with garnet, by small amounts of melting, and that ER106 was formed later than the rest by larger, but still small, amounts of melting after garnet was no longer stable. .

This is consistent with the decreasing ratio of $(Ce/Nd)_N$ in the sequence from ER117 to ER106. Subsequent low pressure fractionation of these primary liquids did not affect the IE ratios.

This sequence of melting is also supported by the variation of other incompatible elements, such as Ti and Zr, with the change in wt. percent of MgO (Figs. 14 a&b). The earlier liquids produced were more enriched in these elements than later liquids. Thus, a Ti and Zr enriched phase must have been one of the first to enter the melt. As melting progressed, the content of these elements became diluted in the melt while the MgO content increased.

ER107 is intermediate in major and trace element composition between the tholeiite series and the komatiite series. Mass balance calculations (Appendix III) were done using an average tholeiite composition and an average composition of the ultramafic rocks produced by partial melting. The proportions of liquids were determined by using the trace element variation diagrams. For all elements, these calculations reveal that a rock with the composition of ER107 can be produced by mixing 25-30% of the komatiitic liquid with 70-75% of the tholeiitic liquid. This mechanism could explain why ER107 lies above

the field of tholeiites on the olivine saturation diagram (Fig. 12) and why it has a slightly enriched ((Ce/Nd)>1) fractionated pattern (Fig. 6).

In summary the tholeiitic rocks can be related by small (<10%) degrees of partial melting of a depleted chondritic pyrolite (garnet lherzolite) source with fractional crystallization superimposed on the melting process. The high-Mg tholeiite may be a mixture of tholeiitic and komatiitic liquids.

Gabbroic rocks

The gabbroic rocks have major element compositions similar to those of the tholeiites except that they are slightly higher in Al_2O_3 and significantly higher in CaO. Their Mg numbers (65-69) are close to those for mantle derived rocks. Two gabbros which were analyzed for REE have chondrite normalized patterns (Fig.7) which are flat to slightly HREE depleted and have complementary Eu anomalies. The Eu anomalies suggest a model in which ER116 represents a plagioclase cumulate and ER114 its residual liquid.

The normative mineralogy of these two rocks is consistent with the proposed model. ER116 has 50% normative plagioclase plus pyroxene and olivine whereas ER114 has

only 30% normative plagioclase plus pyroxene and quartz. The other gabbros which were not analyzed for REE have more than 50% normative plagioclase and have slightly lower Mg numbers.

The chemistry can be used to demonstrate the consistency of this model (see Appendix III). To estimate the amount of liquid (X_L) trapped with the cumulate crystals, an element (Cr) was chosen which is the least mobile and most depleted in ER116 with respect to ER114 (ie. that which exists almost exclusively in the liquid). After calculating X_L (=0.25), a mass balance approach was used to estimate the composition of the cumulate assemblage. The normative mineralogy of this composition is: 54.2% plagioclase, 9.0% clinopyroxene, 5.1% orthopyroxene and 30.5% olivine. The chondrite normalized REE abundances of this assemblage were also calculated using mass balance (Fig. 16). Using the calculated normative mineralogy and published Kd's (Arth, 1976), bulk distribution coefficients for the REE were calculated. These D_o values are consistent with the normalized REE abundances calculated by mass balance (see Appendix III).

If this model is valid, the REE composition of the original liquid (C_o) would be flat to slightly LREE enriched with abundances of 6-8xCHON. This is different

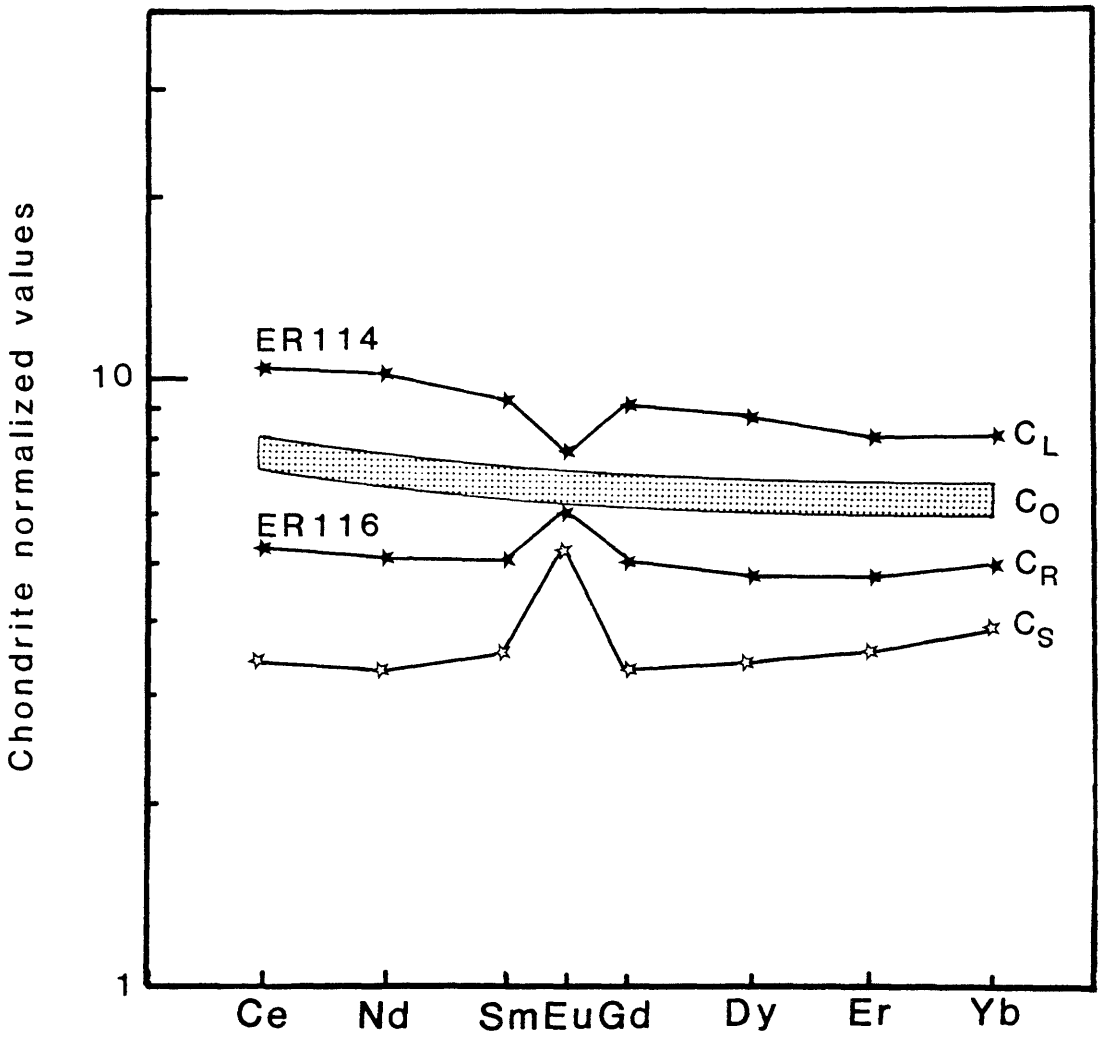

Figure 16.--Calculated model for the possible cumulate and liquid which formed the gabbros.

from both of the other series. The trace element variations (Figs. 4, 14 a&b) also show that these rocks do not correspond to either of the other two series. Mass balance calculations do not support a mixing model for the origin of these rocks. The REE abundances are lower than the tholeiites and the Mg numbers are higher. It is possible that they could have fractionated from similar melts. If this is the case, a difference in conditions must have existed so that the gabbros fractionated plagioclase and the tholeiites were erupted as liquids with no plagioclase accumulation.

Thus, the origin of the gabbros cannot be easily related to the other rocks in the volcanic pile. What they do suggest is that one or more differentiating magma chambers did exist at fairly shallow levels within the sequence.

Metasedimentary rocks

Several types of metamorphosed sedimentary rocks occur within the greenstone belt. Original rock types range from greywacke to marble and banded iron formation. In the portion of the belt under study, three rock types occur which are interpreted to be of sedimentary origin.

One rock type, represented by ER118, was originally

included in the volcanic tholeiite series because of its appearance and spatial association with the tholeiitic amphibolites in the field. However, its chemical composition does not support a volcanic protolith. The high silica and iron may suggest is partially of an exhalative origin. The enrichment of Zr and Nb may be related to crustal sources. The low MgO content and lack of Cr do not support the possibility that this rock may represent an alteration product of the adjacent volcanics. The REE pattern of ER118 is flat and 50 xCHON with small Ce and Eu anomalies (Fig. 8). Anomalies of these elements may be indicative of exposure to alteration processes (Henderson, 1984; Sun & Nesbitt, 1978). The total enrichment of all the REE, compared to other rocks in the vicinity can not be explained at this time. There is too little evidence on which to base any conclusions as to the protolith of this rock.

The other metasedimentary rocks in the belt are typical of greywacke and greywacke conglomerates around the world (Taylor & McLennan, 1981a). The metaconglomerate sample which was not chemically analyzed, has a greywacke matrix and granitic clasts. Greywacke material suggests exposure of both felsic and mafic provinces at the time of deposition (McLennan & Taylor, 1984). The granitic

clasts in the conglomerate are evidence that a granitic (or granitic-gneiss) source was exposed during the formation of the belt. Greywackes and conglomerates in other Archean provinces have been related to deposition by turbidity currents or other mechanisms in relatively deep water on or near subaqueous fans. Some Archean sediments may have formed on land in alluvial fans or braided streams (Ojakangas, 1985). It is difficult to say what the origin of the exposed granitic source was.

ER104 occurs between two tholeiitic units while ER120 is in close proximity to two komatiitic units. The conglomerate, ER115, is in contact with gabbro, tholeiite and komatiitic rocks. The chemistry of these two greywackes is slightly different. ER104 has slightly more SiO_2, MgO and less Al_2O_3 than ER120. The alkali content of these two rocks is quite different. ER120 is slightly enriched in Na_2O. The Rb, Sr, Y and Nb contents of ER104 are much higher than ER120. These chemical differences may be due to a change in source region for the deposition of these rocks. The REE contents of these rocks are remarkably similar however. With the exception of small Eu anomalies, their REE patterns (Fig. 9) are similar to each other and to those of most Archean greywackes (McLennan & Taylor, 1984). The Eu anomalies probably

developed during weathering or sedimentation processes or may reflect an original characteristic of the source rocks. REE patterns of this type are consistent with a source which is a mixture of mafic and felsic rocks (McLennan & Taylor, 1984).

Petrogenetic Relationships

The above discussion has shown that the major rock types in the belt, tholeiites and komatiites, have no apparent genetic relationship to each other. The behavior of the transition metals in these two rock types shows that the tholeiites are compositionally distinct from the komatiites. The gabbros, for the most part, do not relate to either of the other rock types. The break in slope of Co and Cr versus Mg number (Fig. 4) may represent a change in the major fractionating phase within the melts. Cobalt and Cr are more incompatible in olivine, a main crystallizing during formation of the phase which formed the komatiitic rocks, than pyroxene, a main crystallizing phase which formed the tholeiitic rocks (Irving, 1978). Vanadium is incompatible in both the tholeiitic and komatiitic rocks and decreases with the amount of partial melting involved. Vanadium is somewhat incompatible in the gabbros. The spectrum of elements

between the komatiites and tholeiites suggests that the mineralogy of each source may have been similar.

All rocks within a single series can be related to each other by various magmatic processes from a common source. The tholeiites were probably derived by small amounts of partial melting and subsequent fractional crystallization of slightly depleted source while rocks of the komatiitic series were probably derived from an enriched source by various amounts of partial melting and fractional crystallization. The enrichment of this source may be related to a prior metasomatic event, the addition of an enriched liquid to the melt or crustal contamination. Both these magma types were generated at or close to a depth where garnet is stable (>80km). The cumulates of the ultramafic series are probably related to the komatiitic rocks and represent shallow level magma chambers within the volcanic pile of tholeiitic and komatiitic rocks.

The gabbros represent stratified magma chambers which also occured at shallow levels within the pile. They can not be related to the other magmatic rocks in the belt based on the data available at this time. It can be shown that they are texturally and chemically different from these other two rock types. It is possible that they

were derived from a parental liquid similar to the tholeiites,but which fractionated under different conditions which caused plagioclase accumulation in the gabbros, but not the tholeiites.

Not enough is known about the garnetiferous amphibolite to relate it to the other rocks of the suite but, because of its intimate field relationship with the tholeiitic rocks, it may be somehow genetically related to the volcanic activity which produced these rocks.

The metagreywackes and metaconglomerate rocks are sediments derived from a province of both mafic and felsic rocks. Their genetic relationship to the volcanics is uncertain, but their intimate spatial relationships with the volcanic rocks may provide a clue as to the tectonic environment in which the greenstones were formed.

TECTONIC IMPLICATIONS

An interesting task for most geologists who study ancient rocks is to develop a tectonic model which is consistent with the chemical and physical properties of the rocks under study. Debate continues as to whether plate tectonics, as understood today, operated during Archean time. There is controversy as to whether there was a thinner crust or a higher geothermal gradient in the Archean than there is today (Green, 1984; Nisbet, 1984; Burke & Kidd, 1978; Green, 1975) and whether the movement which controlled the geologic environment during the Archean was mostly vertical or more horizontal as is the cases today (Sleep & Windley, 1982; Windley, 1981; Gorman, et al, 1978; Groves, et al, 1978; Anhaeusser, et al, 1969) Caution must be exercised when relating ancient volcanic rocks to those formed in modern environments.

A model for the tectonic environment in which the mafic and ultramafic volcanic pile in the ERGB formed is discussed below. It is based on analogs to modern plate tectonics, keeping in mind that they may or may not be valid for Archean rocks.

The chemical evidence we have suggests an environment which allowed rising mafic and ultramafic diapirs and

near surface magma chambers to exist. Such features would be expected where the crust was thin, such as divergent environments, or in a melting zone above subducted lithosphere in a zone of convergence. The evidence for garnet in equilibrium with both the komatiites and tholeiites suggests that they were generated at significant depths.

Discrimination diagrams for the classification of volcanic environments have been developed by several workers (Meschede, 1986; Briqueu, et al, 1984; Pearce & Norry, 1979; Pearce, et al, 1977; Ewart, 1976; Pearce, 1976; Smith & Smith, 1976; Pearce & Cann, 1973; Jakes & White, 1972; Glikson, 1971; Hart, et al, 1970). Although it may not be proper to compare ancient rocks with those in modern environments these diagrams do identify interesting variations. Those diagrams which may be useful for the classification of ancient environments employ the immobile trace elements Ti, Zr and Cr (Garcia, 1978). When these are applied to ERGB rocks it is not surprising that many of the mafic and ultramafic rocks can be classified as ocean floor basalts (OFB). Using the Ti vs. Cr discrimination diagram (Fig. 17a) only a few samples fall into the island arc tholeiite (IAT) field. On the Ti vs. Zr diagram (Fig. 17b) there is a distinction between the

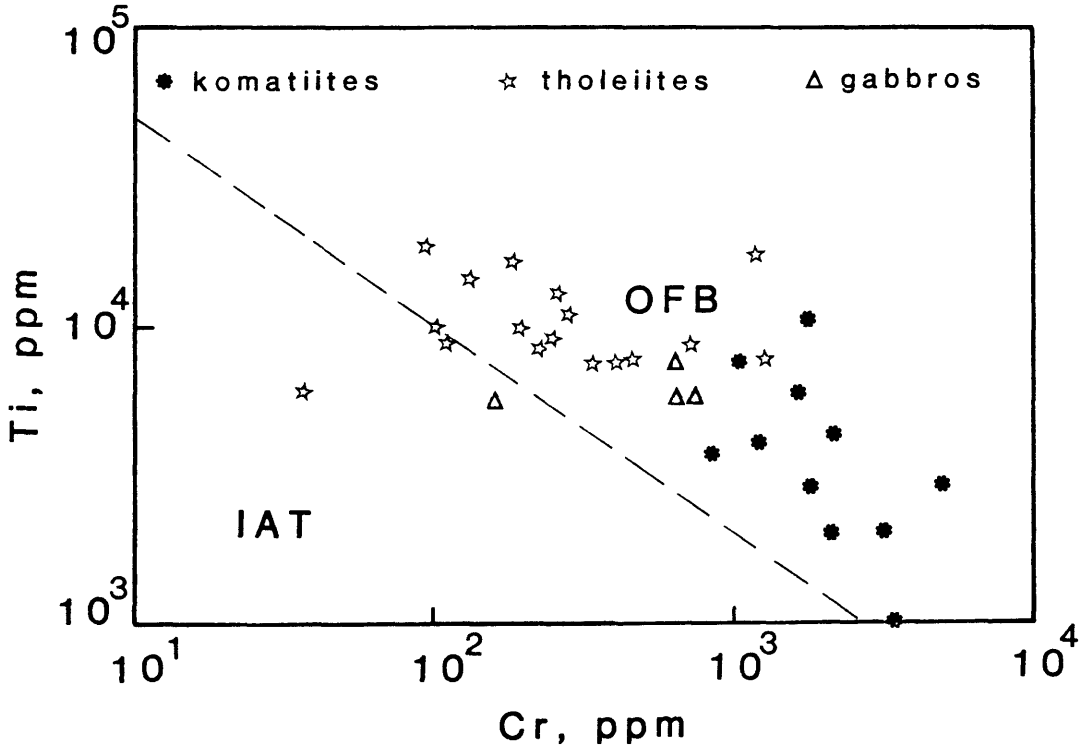

(a) Ti versus Cr

Figure 17.--Discrimination diagrams used to identify possible tectonic environments in which the Elmer's Rock Greenstone Belt may have formed.

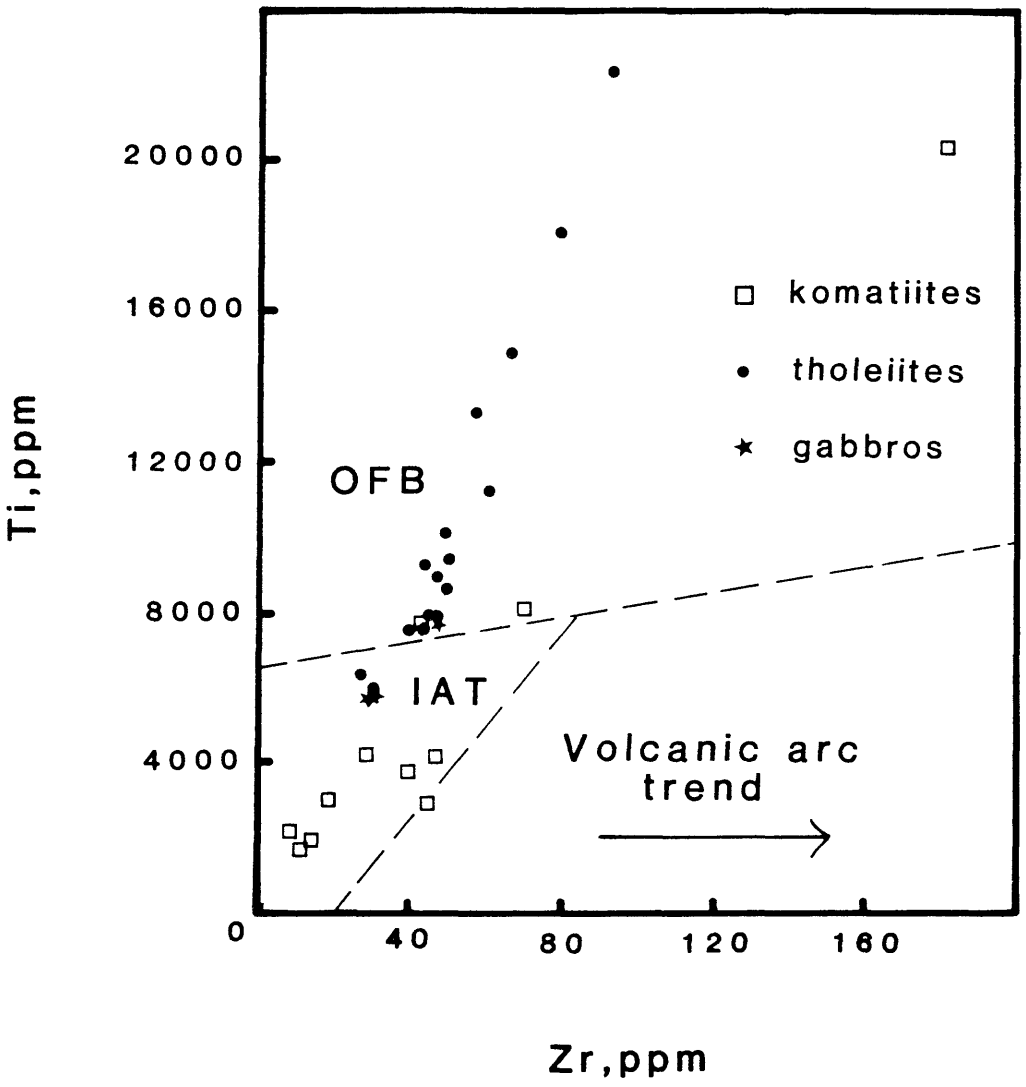

(b) Ti versus Zr

Figure 17.--(con't).

ultramafic rocks, which fall mostly in the IAT field and the mafic rocks, which fall mostly in the OFB field. If these classifications are valid, implications for the tectonic environment of these rocks are that it contains both ocean floor and island arc rocks. Since IAT are the first to form in a new island arc (Ringwood, 1974), it is probable that these rocks formed in the Archean equivalent of a primitive continental margin or near continent island arc. The large clasts in the metaconglomerate suggest a near continent environment.

The criteria for the Elmer's Rock Greenstone Belt which support this type of tectonic setting are: (1) the dominance of mafic-ultramafic rocks in the suite and the transition of the intrusive(?) gabbros toward calc-alkaline compositions argue for an island arc setting (Hawkins, et al, 1984; Basaltic Volcanism Study Project, 1981; Jakes & White, 1972); (2) although calc-alkaline rocks do exist in what is interpreted as the upper portion of the belt (Graff, et al, 1982) , the lack of large quantities of alkali basalts argues against a rift setting (Dupuy & Dostal, 1984; Basaltic Volcanism Study Project, 1981); (3) the occurrence of clastic metasediments within the lower volcanic sequence argues for a convergent environment (Ojakangas, 1985; Sigurdsson, 1982a,

1982b; Dickinson, 1974); (4) major and trace elements of the tholeiites are similar to modern island arc and ocean floor lavas while the komatiitic rocks have chemistry similar to ophiolites and boninites (Cameron, et al, 1979; (Basaltic Volcanism Study Project, 1981; Sun, et al, 1979; Sun & Nesbitt, 1978b) ; (5) the LREE enrichment of the ultramafic magmas argues for the interaction of CO_2-rich fluids with the mantle which can be caused by the melting of subducted lithosphere (Schneider & Eggler, 1986; Lloyd & Bailey, 1975); (6) the temperature and pressure conditions required to produce high-Mg rocks (Herzberg, et al, 1986; Cox, 1978; Arndt, 1977; Arndt, 1976; 1976; Green, 1975) are not characteristic of divergent settings (Basaltic Volcanism Study Project, 1981) ; and, (7) the REE patterns of many of these rocks supports equilibrium with garnet which implies significant depths of generation (Jaques & Green, 1980; Ringwood, 1975).

The pressure and temperature conditions necessary to produce these rocks are possible in a convergent tectonic setting. High Mg (komatiitic) rocks are believed to form from high degrees of partial melting at moderate mantle depths at high temperatures (Green, 1975, 1981) or by small degrees of partial melting at greater depths (Herzberg, et al, 1986; Ohtani, 1984; Takahashi, 1981).

Subduction of a lithospheric plate may initiate melting in the mantle at depths near 200 km (Ernst, 1987). Small amounts of melting of an IE-enriched garnetiferous source at such depths would produce ultramafic magmas (Ohtani, 1984) such as those found in the ERGB. Melting of the same source at depths between 80 and 100 km would produce tholeiitic magmas (Takahashi & Kushiro, 1983; Ringwood, 1974). Melting may be aided by the subduction of a spreading center or mantle plume which would increase heat flow in the subduction zone. Such phenomena may have been common in the Archean.

Our interpretations suggest that the magmas which produced the volcanic rocks of the ERGB resulted from low to moderate degrees of melting. While the tholeiitic and komatiitic liquids were probably produced from two distinct sources, both series have some rocks which were in equilibrium with garnet and some which were not. Rising mantle diapirs may be the most consistent explanation for the generation mechanism of these rocks. Rising diapirs are thought to occur in both divergent environments and in a melting zone above a subducting lithospheric slab. If the diapirs are large, the magmas from the lower part of the diapir would be in equilibrium with garnet while those in the upper part would not. An environment which

allows rising diapirs may also allow for the mixing of liquids, such as those which produced ER107. The tectonic environment which is most consistent with our model is that of a primitive island arc or continental margin setting.

SUMMARY

Evaluation of the data obtained from the Elmer's Rock Greenstone Belt rocks has produced a simple and consistent model for the petrogenesis of the magmas which formed this volcanic suite and set some limits on the tectonic environment in which they formed:

1) The mafic and ultramafic rocks from ERGB represent a volcanic pile of tholeiites, komatiites and komatiitic basalts interbedded with intrusive (?) gabbros and sediments, which compare with many other greenstone belts, both Archean and younger (Table 3).

2) Some of the ultramafic rocks in the suite represent cumulates from the komatiitic series.

3) The magmas which formed the komatiitic and tholeiitic rocks were derived from sources which have had significantly different histories; the source for the komatiitic rocks was enriched in LREE and other IE while the source for the tholeiites was slightly depleted in LREE with no significant variation in other trace elements.

4) The LREE enrichment of the komatiitic source may be related to metasomatic alteration of the source before melting; mixture of strongly IE enriched fluids with the melt; or contamination by crustal material during ascent.

5) The formation of the komatiitic rocks can be

related to direct partial melting of a garnetiferous source, in moderate degrees (10-40%), to form komatiites and komatiitic basalt along with fractional crystallization of the komatiite liquid to produce komatiitic basalt; The tholeiites were probably formed by low degrees of partial melting of a garnetiferous pyrolite source and subsequent fractional crystallization of the melt.

6) The interpretation that some of these melts were in equilibrium with garnet while others were not can be best explained by the existence of large rising diapirs under which different pressure and temperature conditions existed (ie, melts generated at greater depths by smaller amounts of melting would be in equilibrium with garnet while melts generated by larger amounts of melting or at shallower depths would not).

7) Sedimentary rocks in the belt may represent both clastic and exhalative environments; the greywackes and conglomerate are consistent with the exposure of mafic and felsic rocks in the area of deposition.

8) Tectonic implications suggest that the Elmer's Rock Greenstone Belt probably formed during the early stages of formation of an island arc or continental margin.

REFERENCES CITED

ABBEY, S., 1975, Studies in "Standard Samples" of silicate rocks and minerals; in: "Usable" values, part 4, 1974 ed., Geological Survey Paper 74-41, p. 1.

AITKEN, B.G., ECHVERRIA, L.M., 1984, Petrology and geochemistry of komatiites and tholeiites from Gorgona Island, Columbia; Contrib. Min. Pet., v. 86, pp. 94-105.

ALLEGRE, C.J., MINSTER, J.F., 1978, Quantitative models of trace element behavior in magmatic processes; Earth Plan. Sci. Lett., v. 38, pp. 1-25.

ANHAESSER, C.P., MASON, R., VILJOEN, M.J., VILJOEN , R.P., 1969, A reappraisal of some aspects of Precambriam geology; G.S.A. Bulletin, v. 80, pp. 2175-2200.

APTED, M.J., 1981, Rare earth element systematics of hydrous liquids from partial melting of basaltic eclogite: a re-evaluation; Earth Plan. Sci. Lett., v. 52, pp. 172-182.

ARNDT, N.T., 1986, Differentiation of komatiite flows, J. Petrol., v. 27, pp. 279-301.

-----, JENNER, G., 1986, Crustally contaminated komatiites and basalts from Kambalda, W. Australia; Chem. Geol., v. 55, pp. .

-----, NISBET, E.G., (eds.), 1982a, Komatiites; George Allen & Unwin, Boston, 526 p.

-----, -----, 1982b, What is a komatiite?; in Komatiites, N.T. Ardnt & E.G. Nisbet, eds., George Allen & Unwin, Boston, pp. 19-28.

-----, 1977, Ultrabasic magmas and high degree melting of the mantle; Contrib. Min. Pet., v. 64, pp. 205-221.

-----, 1976, Melting relations of ultramafic lavas (komatiites) at one atmosphere and high pressure; Carnegie Inst. Wash., yearbook, v. 75, pp. 555-561.

ARTH, J.G., 1976, Behavior of trace elements during magmatic processes - A summary of theoretical models and their applications; Jour. Research U.S. Geol. Surv., v. 4, pp.41-47.

-----, ARNDT, N.T., NALDRETT, A.J., 1977, Genesis of Archean komatiites - trace element evidence from Munro Township, Ontario; Geology, v. 5, pp. 590-594.

BARLEY, M.E., 1986, Incompatible-element enrichment in Archean basalts: A consequence of contamination by older sialic crust rather than mantle heterogeneity; Geology, v. 14, pp. 947-950.

BASALTIC VOLCANISM STUDY PROJECT, 1981, Basaltic Volcanism on the Terrestrial Planets; Pergamon Press, New York, 1286 p.

BESWICK, A.E., 1982, Some geochemical aspects of alteration and genetic relations in komatiitic suites; in Komatiites, N.T. Ardnt & E.G. Nisbet, (eds), George Allen & Unwin, Boston, pp. 283-308.

BESWICK, A.E., SOUCIE, G., 1978, A correction procedure for metasomatism in an Archean greenstone belt; Precambrian Res., v. 6, pp. 235-248.

BICKLE, M.J., HAWKESWORTH, C.J., MARTIN, A., NISBET, E.G., O'NIONS, R.K., 1976, Mantle composition derived from the chemistry of ultramafic lavas; Nature, v. 263, pp. 577-580.

BINNS, R.A., HALLBERG, J.A., TAPLIN, J.H., 1982, Komatiites in the Yilgarn Block, Western Australia; in Komatiites, Arndt & Nisbit (eds), George Allen & Unwin, Boston, pp. 117-130.

BOWER, N.W., 1985, Optimization of precision and accuracy in x-ray fluorescence analysis of silicate rocks; App. Spectr., v. 39, pp. 697-703.

BOWER, N.W., VALENTINE, G., 1986, Critical comparison of sample preparation methods for major and trace element determinations using x-ray fluorescence; X-ray Spectr., v. 15, pp. 73-78.

BRIQUEU, L., BOUGAULT, H., JORON, J.L., 1984, Quantification of niobium, tantalum, titanium and vanadium anomalies in magmas associated with subduction zones: petrogenetic implications; Earth Plan. Sci. Lett., v. 68, pp. 297-308.

BURKE, K., KIDD, W.S.F., 1978, Were Archean continental geothermal gradients much steeper than those of today?;

Nature, v. 272, pp. 240-241.

CAMERON, W.E., NISBET, E.G., DIETRICH, V.J., 1979, Boninites, komatiites and ophiolitic basalts; Nature, v.280, pp. 550-553.

CARMICHEAL, I.S.E., TURNER, F.J., VERHOOGAN, J., 1974, Igneous Petrology; McGraw-Hill, New York, 739p.

CAWTHORN, R.G., STRONG, D.F., 1975, The petrogenesis of komatiites and related rocks as evidence for a layered upper mantle; Earth Plan. Sci. Lett., v. 27, pp. 369-375.

COMPSTON, W., WILLIAMS, I.S., CAMPBELL, I.H., GRESHAM, J.J., 1986, Zircon xenocrysts from the Kambalda volcanics: Age constraints and direct evidence for older continental crust below the Kambalda-Norseman greenstones; Earth Plan. Sci. Lett., v. 76, pp. 299-311.

CONDIE, K.C., 1981, Archean Greenstone Belts, Elsevier, New York, 434 p.

-----, VILJOEN, M.J., KABLE, E.J.D., 1977, Effects of alteration on element distribution in Archean tholeiites from Barberton greenstone belt, South Africa; Contrib. Min. Pet., v. 64, pp. 75-90.

-----, 1976, Trace-element geochemistry of Archean greenstone belts; Earth. Sci. Rev., v. 12, pp. 393-417.

-----, 1976, The Wyoming Archean Province in the western United States; in B.F. Windley (ed.), The Early History of the Earth, J. Wiley & Sons, New York, pp. 499-510.

-----, 1967, Geochemistry of early Precambrian greywackes from Wyoming; Geochim. Cosmochim. Acta, v. 31, pp. 2135-2149.

COX, K.G., 1978, Komatiites and other high-magnesia lavas: some problems; Philos. Trans. R. Soc. London, Ser. A, v. 288, pp. 599-609.

DICKINSON, W.R., 1974, Sedimentation within and beside ancient and modern magmatic arcs; in R.H. Dott & R.H. Shaver (eds), Modern and Ancient Geosynclinal Sedimentation, S.E.P.M., Spec. Pub., n. 19, pp. 230-239.

DIETRICH, V.J., GANSSER, A., SOMMERAUER, J., CAMERON, W.E., 1981, Paleogene komatiites from Gorgona Island, East

Pacific - a primary magma for ocean floor basalts?; Geochem. J., v. 15, pp. 141-146.

DUNCAN, R.A., GREEN, D.H., 1980, Role of multistage melting in the formation of oceanic crust; Geology, v. 8, pp. 22-26.

DUPUY, C., DOSTAL, J., 1984, Trace-element geochemistry of some continental tholeiites; Earth Plan. Sci. Lett., v. 67, pp. 61-69.

ECHEVERRIA, L.M., 1982 Komatiites from Gorgona Island, Columbia; in Komatiites, Arndt & Nisbet, (eds), George Allen & Unwin, Boston, pp. 199-209.

ERIKSSON, C.,1987, Petrology of the alkalic hypabyssaland volcanic rock at Cripple Creek, Colorado; M.S. thesis, Colorado School of Mines, 114 p.

ERNST, W.G., 1987, Mafic meta-igneous rocks of apparent komatiitic affinities, Sawyers Bar area, central Klamath Mountains, northern California; in B.O. Mysen (ed), Magmatic Processes: Physiochemical Principles, The Geochemical Society, Spec. Pub., n. 1, pp. 191-208.

EWART, A., 1976, Mineralogy and chemistry of modern orogenic lavas - some statistics and implications; Earth Plan. Sci. Lett., v. 31, pp. 417-432.

FORD, C.E., RUSSELL, D.G., CRAVEN, J.A., FISK, M.R., 1983, Olivine-liquid equilibria: Temperature, pressure and composition dependence of the crystal/liquid partition coefficients for Mg, Fe^{2+}, Ca and Mn; J. Petrol., v. 24, pp. 256-265.

FREY, F.A., GREEN, D.H., ROY, S.D., 1978, Integrated models of basalt petrogenesis: a study of quartz tholeiites to olivine melilites from southeastern Australia utilizing geochemical and experimental petrologic data; J. Petrol., v. 19, pp. 463-513.

FUJIMAKI, H., TATSUMOTO, M., AOKI, K., 1984, Partition coefficients of Hf, Zr and REE between phenocrysts and ground mass; J. Geophys. Res., B., v. 89 (Suppl.), pp. 662-672.

GAST, P.W., 1968, Trace element fractionation and the origin of tholeiitic and alkaline magma types; Geochim.

Cosmochim. Acta, v. 32, pp. 1057- .

GARCIA, M.O., 1978, Criteria for the identification of ancient volcanic arcs; Earth Sci. Rev., v. 14, pp. 147-165.

GILL, R.C.O., 1979, Comparative petrogenesis of Archean and modern low-K tholeiites: a critical review of some geochemical aspects; Phys. Chem. Earth, v. 11, pp. 431-447.

GLIKSON, A.Y., 1971, Primitive Archean element distribution patterns: chemical evidence and geotectonic significance; Earth Plan. Sci. Lett., v. 12, pp. 309-320.

GOLDICH, S.S., 1984, Determination of ferrous iron in silicate rocks; Chem. Geol., v. 42, pp. 343-347.

GORMAN, B.E., PEARCE, T.H., BIRKETT, T.C., 1978, On the structure of Archean greenstone belts; Precambrian Res., v. 6, pp. 23-41.

GRAFF, P.J., SEARS, J.W., HOLDEN, G.S., HAUSEL, W.D., 1982, Geology of the Elmer's Rock Greenstone Belt, Laramie Range, Wyoming; Geol. Surv. Wyo., Rept. Inv. No. 14, 23 p.

GREEN, D.H., 1984, Petrogenesis of Archean ultramafic magmas and implications for Archean tectonics; in Precambrian Plate Tectonics, Chapter 19, Elsevier, Amsterdam , pp. 469-490.

-----, 1975, Genesis of Archean peridotitic magmas and constraints on Archean geothermal gradients and tectonics; Geology, v. 3, pp. 15-18.

-----, PEARSON, N.J., 1986, Ti-rich accessory phase saturation in hydrous mafic-felsic compositions at high pressure and temperature; Chem. Geol., v. 54, pp. 185-201.

-----,-----, 1985, Rare earth element partitioning between clinopyroxene and silicate liquid at moderate to high pressure; Contrib. Min. Pet., v. 91, pp. 24-36.

GROVES, D.I., KORKIAKOSKI, E.A., McNAUGHTON, N.J., LESHER, C.M., COWDEN, A., 1986, Thermal erosion by komatiites at Kambalda, W. Australia, and the genesis of nickel ores; Nature, v. 319, pp. 136-139.

-----, ARCHIBALD, N.J., BETTENAY, L.F., BINNS, R.A., 1978,

Greenstone belts as ancient marginal basins or ensialic rift zones; Nature, v. 273, pp. 460-461.

HANSON, G.N., 1981, Geochemical constraints on the evolution of the early continental crust; Phil. Trans. R. Soc. Lond., v. A301, pp. 423-442.

-----, 1980, Rare earth elements in petrogenetic studies of igneous systems; Ann. Rev. Earth Plan. Sci., v. 8, pp. 371-406.

HANSON, G.N., LANGMUIR, C.H., 1980, Modelling of major elements in mantle-melt systems using trace element approaches; Geochim. Cosmochim. Acta, v. 42, pp. 725-741.

HART, S.R., BROOKS, C., KROUGH, T.E., DAVIS, G.L., NAVA, D., 1970, Ancient and modern volcanic rocks: A trace element model; Earth & Plan. Sci. Lett., v. 10, pp. 17-28.

HAWKESWORTH, C.J., O'NIONS, R.K., 1977, The petrogenesis of some Archean volcanic rocks from southern Africa; J. Petrol., v. 18, pp. 487-520.

HAWKINS, J.W., BLOOMER, S.H., EVANS, C.A., MELCHIOR, J.J., 1984, Evolution of intra-oceanic arc-trends systems; Tectonophysics, v. 102, pp. 175-205.

HENDERSON, P., (ed), 1984, Rare Earth Element Geochemistry, Developments in Geochemistry, v. 2; Elsevier, New York, 510 p.

HERMANN, A.G., BLANCHARD, D.P., HASKIN, L.A., JACOBS, J.W., KNAKE, D., KORSTER, R.L., BRANNON, J.C., 1976, Major, minor and trace element compositions of peridotitic and basaltic komatiites from the Precambrian crust of southern Africa; Contrib. Min. Pet., v. 59, pp. 1-12.

HERZBERG, G.T., HASEBE, K., SAWAMOTO, H., 1986, Origin of high Mg komatiites: constraints from melting experiments to 8GPa (abs); Trans. Amer. Geophys. Union, v. 67, p. 408.

HILLS, F.A., ARMSTRONG, R.L., 1974, Geochronology of Precambrian rocks in the Laramie Range and implications for the tectonic framework in southern Wyoming; Precambrian Research, v. 1, p. 213-225.

HUMPHRIS, S.E., 1984, The mobility of rare earth elements in the crust; in Henderson, P., (ed), REE Geochemistry,

Chap. 9, Elsevier, Amsterdam, pp. 317-373.

-----, THOMPSON, G., 1978, Trace element mobility during hydrothermal alteration of oceanic basalts; Geochim. Cosmochim. Acta, v. 42, pp. 127-136.

-----, -----, 1978, Hydrothermal alteration of oceanic basalts by sea-water; Geochim. Cosmochim. Acta, v. 42, pp. 107-125.

-----, MORRISON, M.A., THOMPSON, R.N., 1978, Influence of rock crystallization history on subsequent lanthanide mobility during hydrothermal alteration of basalts; Chem. Geol., v. 23, pp. 125-137.

HUPPERT, H.E., SPARKS, R.S.J., 1985a, Cooling and contamination of mafic and ultramafic magmas during ascent through continental crust; Earth Plan. Sci. Lett., v. 74, pp. 371-386.

-----, -----, 1985b, Komatiites 1: Eruption and flow; J. Petrol., v. 26, pp. 694-725.

IRVING, A.S., 1978, A review of experimental studies of crystal/liquid trace element partitioning; Geochim,=. Cosmochim. Acta, v. 42, pp. 743-770.

JAHN, B.-M., AUVAY, B., BLAIS, S., CAPDEVILA, R., CORNICHET, J., VIDAL, F., HAMEUR, J., 1981, Trace element geochemistry and petrogenesis of Finnish greenstone belts; J. Petrol., v. 21, pp. 201-244.

-----, SHIH, C.-Y., MURTHY, V.R., 1974, Trace element geochemistry of Archean volcanic rocks; Geochim. Cosmochim. Acta, v. 38, pp. 611-627.

JAKES, P., WHITE, A.J.R., 1972, Major and trace element abundances in volcanic rocks of orogenic areas; G.S.A. Bull., v. 83, pp. 29-39.

JAQUES, A.L., GREEN, D.H., 1980, Anhydrous melting of peridotite at 0-15 Kb pressure and the genesis of tholeiitic basalts; Contrib. Min. Petrol., v. 73, pp. 287-310.

JENSEN, L.S., 1976, A method of classifying subalkalic volcanic rocks; Ontario Div. Mines, Misc. Paper 66, 22p.

KUSHIRO, I., 1975, On the Nature of silicate melt and its significance in magma genesis: Regularities in the shift

of the liquidus boundaries involving olivine, pyroxene and silica minerals; Am. J. Sci., v. 275, pp. 411-431.

-----, 1972, Effect of water on the composition of magmas at high pressures; J. Petrol., v. 13, pp. 311-334.

LAMBERT, D.D., 1982, Geochemical evolution of the Stillwater Complex, Montana: evidence for the formation of platinum-group element deposits in mafic layered intrusions; Ph.D. thesis, Colorado School of Mines, 274p.

LANGMUIR, C.H., HANSON, G.N., 1981, Calculating mineral-melt equiliria with stoichiometry, mass balance and single component distribution coefficients; Adv. Phys. Geochem., v. 1, pp. 247-271.

LLOYD, F.E., BAILEY, D.K., 1975, Light element metasomatism of the continental mantle: the evidence and consequence; in L.H. Ahrens, et al, (eds), Phys. Chem. Earth, v. 9, pp. 389-416.

LUDDEN, J.N., THOMPSON, G., 1979, An evaluation of the behavior of the rare earth elements during the weathering of sea-floor basalt; Earth Plan. Sci. Lett., v. 43, pp. 85-92.

-----, -----, 1978, Behavior of REE during submarine weathering of tholeiitic basalt; Nature, v. 274, pp. 147-149.

-----, HUMPHRIS, S.E., 1978, Are the REE mobile during alteration processes?; G.S.A. Abstr. Prog, v. 10, p. 447.

-----, GELINAS, L., TRUDEL, P., 1982, Archean metavolcanics from Rouyn-Noranda district, Abitibi Greenstone Belt, Quebec (Canada)2. Mobility of trace elements and petrogenetic constraints; Can. J. Earth Sci., v. 19, pp. 2276-2287.

-----,-----, 1982, Trace element charcateristics of komatiites and komatiitic basalts from the Abitibi metavolcanic belt of Quebec; in Komatiites, Arndt & Nisbet (eds), Geogre Allen & Unwin, pp. 309-330.

MARSTON, R.J., 1978, The geochemistry of the Archean clastic metasediments in relation to crustal evolution, northeastern Yilgarn block, W. Australia; Precambrian Res., v. 6, pp. 157-175.

McLENNAN, S.M., TAYLOR, S.R., 1984, Archean sedimentary rocks and their relation to the composition of the Archean continental crust; in Archean Geochemistry, Kroner, et al, (eds), Springer-Verlag, New York, pp. 47-72.

MENZIES, M., BLANCHARD, D., JACOBS, J., 1977, Rare earth and trace element geochemistry of metabasalts from the Point Sal ophiolite, California; Earth Plan. Sci. Lett., v. 37, pp. 203-215.

MESCHEDE, M., 1986, A method of discriminating between different types of mid-ocean ridge basalts and continental tholeiites with the Nb-Zr-Y diagram; Chem. Geol., v. 56, pp. 207-218.

MORRISON, M.A., 1978, The use of "immobile" trace elements to distinguish the paleotectonic affinities of metabasalts: Applications to the Palaeocene basalts of Mull and Skye; Earth Plan. Sci. Lett., v. 39, pp. 407-416.

MYSEN, B.O., 1979, Trace-element partitioning between peridotite minerals and water-rich vapor: experimental data from 5 to 30 kbar; Am. Min., v. 64, pp. 274-287.

NALDRETT, A.J., ARDNT, N.T., 1976, Volcanogenic nickel deposits with some guides for exploration; Trans. Soc. Mining Eng., v. 260, pp. 13-15.

NANCE, W.B., TAYLOR, S.R., 1977, Rare earth element patterns and crustal evolution - II. Archean sedimentary rocks from Kalgoolie Australia; Geochim. Cosmochim. Acta, v. 41, pp. 225-231.

NESBITT, R.W., SUN, S.-S., PURVIS, A.C., 1979, Komatiites: geochemistry and genesis; Can. Mineral. v. 17, pp. 165-186.

-----, -----, 1976, Geochemistry of Archean spinifex-textured peridotites and magnesian and low-magnesian tholeiites; Earth Plan. Sci. Lett., v. 31, pp. 433-453.

NEUMANN, H., MEAD, J., VITALIANO, C.J., 1954, Trace element variation during fractional crystallization as calculated from the distribution law; Geochim. Cosmochim. Acta, v. 6, pp. 90-99.

NISBET, E.G., 1984, The continental and oceanic crust and lithosphere in the Archean; Isostatic, thermal and tectonic models; Can. J., Earth Sci., v. 21, pp. 1426-1441.

-----, CHINNER, G.A., 1981, Controls of the eruption of mafic and ultramafic lavas, Ruthwell Ni-Cu prospect, West Pilbara; Econ. Geol., v. 76, pp. 1729-1735.

OHTANI, E., 1984, Generation of komatiitic magma and gravitational differentiation in the deep upper mantle; Earth Plan. Sci. Lett., v. 67, pp. 261-272.

OJAKANGAS, R.W., 1985, Review of Archean clastic sedimentation, Canadian shield: Major felsic volcanic contributions to turbidite and alluvial fan - fluvial facies associations; in Evolution of Archean Supracrustal Sequences, L.D. Ayres, P.C. Thurston, K.D. Card & W. Weber (eds), Geol. Assn. Can. Spec. Paper 28, pp. 23-48.

O'NIONS, R.K., EVENSEN, N.M., HAMILTON, P.J., 1979, Geochemical modelling of mantle differentiation and crustal growth; J. Geophys. Res., v. 84, pp. 6091-6101.

PEARCE, J.A., NORRY, M.J., 1979, Petrogenetic implications of Ti, Zn, Y and Nb variations in volcanic rocks; Contrib. Min. Pet., v. 69, pp. 33-47.

-----, GORMAN, B.E., BIRKETT, T.C., 1977, The relationship between major element chemistry and tectonic environment of basic and intermediate volcanic rocks; Earth Plan. Sci. Lett., v. 36, pp. 121-132.

-----, 1976, Statistical analysis of major element patterns in basalts; J. Petrol., v. 17, pp. 15-43.

-----, CANN, J.R., 1973, Tectonic setting of basic volcanic rocks determined using trace element analysis; Earth Plan. Sci. Lett., v. 19, pp. 290-300.

PETERMAN, Z.E., HILDRETH, R.A., 1977, Reconnaissance geology and geochronology of the Granite Mountains, Wyoming; USGS, Open File Report 77-140, 86p.

RAJAMANI, V., SHIVKUMAR, K., HANSON, G.N., SHIREY, S.B., 1985, Geochemistry and petrogenesis of amphibolites, Kolar Schist Belt, South India: Evidence for komatiitic magma derived by low percentages of melting of the mantle; J. Petrol., v. 26, pp. 92-123.

RINGWOOD, A.E., Composition and petrology of the Earth's mantle; McGraw-Hill International Series in the Earth & Planetary Sciences, New York, 618pp.

ROEDER, P.L., EMSLIE, R.F., 1970, Olivine-liquid equilibrium; Contrib. Min. Pet., v. 29, pp. 275-289.

SCHILLING, J.-G., 1966, Rare earth fractionation in Hawaiian volcanic rocks; Ph.D. thesis, Mass. Inst. Tech., Cambridge, MA.

SCHNEIDER, M.E., EGGLER, D.H., 1986, Fluids in equilibrium with peridotite minerals: Implications for mantle metasomatism; Geochim. Cosmochim. Acta, v. 50, pp. 711-724.

SCHNETZLER, C.C., PHILPOTTS, J.A., 1970, Partition coefficients of REE between igneous matrix material and rock-forming mineral phenocrysts - II; Geochim. Cosmochim. Acta, v. 34, pp. 331-340.

SCHULZ, K.J., 1982, Magnesian basalts from the Archean terrains of Minnesota; in Komatiites, N.T. Arndt & E.G. Nisbet (eds), George Allen & Unwin, Boston, pp. 171-186.

SIGURDSSON, H., 1982a, Volcanic sediments in island arcs; in L.D. Ayres (ed), Geol. Assn. Can., Short Course Notes, v. 2, pp. 221-293.

-----, 1982b, Subaqueous volcanogenic sediments in oceanic basins; in L.D. Ayres (ed), Geol. Assn. Can., Short Course Notes, v. 2, pp. 294-342.

SLEEP, N.H., WINDLEY, B.F., 1982, Archean plate tectonics: constraints and inferences; J. Geol., v. 90, pp. 363-379.

SMITH, H.S., ERLANK, A.J., 1982, Geochemistry and petrogenesis of komatiites from the Barberton greenstone belt, South Africa; in Komatiites, Arndt & NIsbet (eds.), George Allen & Unwin, Boston, pp. 347-398.

SMITH, R.E., SMITH, S.E., 1976, Comments on the use of Ti, Zr, Y, Sr, K, P and Nb in classification of basaltic magmas; Earth Plan. Sci. Lett., v. 32, pp. 114-120.

SNYDER, G.A., 1986, A Nd and Sr isotopic and trace element study of a mafic-ultramafic dike swarm, Laramie Range, WY; Evidence for Late Archean-Early Proterozoic rifting of the Wyoming Craton; M.S. thesis, Colorado School of Mines, 135p.

SNYDER, G.L., 1984, Preliminary geologic maps of the central Laramie Mountains, Albany and Platte Counties, Wyom-

ing; USGS, Open File Report 84-358, Parts A and D.

SPARKS, R.S.J., 1986, The role of crustal contamination in magma evolution through geological time; Earth Plan. Sci. Lett., v. 78, pp. 211-223.

SPERA, J., 1981, Carbon dioxide in igneous processes: II. Fluid dynamics of mantle metasomatism; Contrib. Min. Pet., v. 77, pp. 56-65.

STONE, W.E., 1986, An unusual Fe-rich Al-depleted komatiite from the Abitibi greenstone belt; Geol. Assn. Can., Abstr. Prog., v. 11, p. 132.

STRAMATELOPOULOU-SEYMOUR, K., FRANCIS, D., LUDDEN, J., 1983, The petrogenesis of the Lac Guyer komatiites and basalts and the nature of the komatiite-komatiitic basalt compositional gap; Contrib. Min. Pet., v. 84, pp. 6-14.

SUN, S.-S., 1984, Geochemical characteristics of Archean ultramafic and mafic volcanic rocks: Implications for mantle composition and evolution; in Archean Geochemistry, Kroner, et al, (eds), Springer-Verlag, New York, pp. 25-46.

SUN, S.-S., NESBITT, R.W., SHARASKIN, A.Y., 1979, Geochemical characteristics of mid-ocean ridge basalts; Earth Plan. Sci. Lett., v. 44, pp. 119-138.

-----, -----, 1978a, Petrogenesis of Archean ultrabasic and basic volcanics: evidence from rare earth elements; Contrib. Min. Pet., v. 65, pp. 301-325.

-----, -----, 1978b, Geochemical regularities and genetic significance of ophiolitic basalts; Geology, v. 6, pp. 689-693.

TAKAHASHI, E., 1986, Melting of a dry peridotite KLB-1 up to 14 GPa: implications on the origin of peridotite upper mantle; J. Geophys. Res., v. 91, pp. 9367-9382.

-----, KUSHIRO, I., 1983, Melting of a dry peridotite at high pressures and basalt magma genesis; Am. Min., v. 68, pp. 859-879.

TARNEY, J., WINDLEY, B.F., 1981, Marginal basins through geologic time; Philos. Trans. R. Soc. London, v. A301, pp. 217-232.

TAYLOR, S.R., MCLENNAN, S.M., 1981a, The compositon and evolution of the continental crust: REE evidence from sedimentary rocks; Philos. Trans. R. Soc. London, v. A301, pp. 381-399.

-----, -----, 1981b, The rare earth evidence in Precambrian sedimentary rocks: Implications for crustal evolution; in A. Kroner, Archean Geochemistry, Springer-Verlag, New York, pp. 527-548.

VILJOEN, M.J., VILJOEN, R.P., 1969, Evidence for the existence of a mobile extrusive peridotitic magma from the Komati Formation of the Onverwacht Group; Geol. Soc. S. Afr. Spec. Publ., pp. 87-112.

VILJOEN, R.P., VILJOEN, M.J., 1969, The geological and geochemical significance of the upper formations of the Onverwacht Group; Geol. Soc. S. Afr. Spec. Publ., pp. 113-152.

WASS, S.Y., RODGERS, N.W., 1980, Mantle metasomatism, precursor to continental alkaline volcanism; Geochim. Cosmochim. Acta, v. 44, pp. 1811-1824.

-----, HENDERSON, P., ELLIOT, C.J., 1980, Chemical heterogeneity and metasomatism in the upper mantle: evidence from rare-earth and other elements in apatite-rich xenoliths in basaltic rocks from eastern Australia; Philos. Trans. R. Soc. London, v. A297, pp. 333-346.

WENDLANDT, R.F., HARRISON, W.J., 1979, Rare earth partitioning between immiscible carbonate and silicate liquids and CO_2 vapor: Results and implications for the formation of LREE-enriched rocks; Contrib. Min. Pet., v. 69, pp. 409-419.

WHITFORD, D.J., ARNDT, N.T., 1978, Rare earth element abundances in a thick, layered komatiite lava flow from Ontario, Canada, Earth Plan. Sci. Lett., v. 41, pp. 188-196.

WINDLEY, B.F., 1981, Precambrian rocks in the light of the plate tectonic concept; in Kroner, A. (ed), Precambrian Plate Tectonics, Elsevier, Amsterdam, pp. 1-20.

WINKLER, H.G.F., 1979, Petrogenesis of Metamorphic Rocks, 5th edition; Springer-verlag, New York, 348 p.

WYLLIE, P.J., 1984, Constraints imposed by experimental

petrology on possible and impossible magma sources and products; Philos. Trans. R. Soc. London, v. A310, pp. 439-456.

-----, 1979, Magmas and volatile components; Am. Min., v. 64, pp. 469-500.

APPENDIX I -- ANALYTICAL PROCEDURES

Sample Collection and Preparation

The ER1XX set of samples was collected and prepared so as to be the most representative samples possible. Five to ten kilograms of the freshest possible hand-sized specimens were collected in the field. Each sample was broken into approximately 1 cm pieces and visually weathered pieces were discarded. The samples were split using a large aluminum splitter which could accommodate the 1 cm pieces. The samples were split and mixed twice. They were then split until 500g portions of the samples remained. These portions were crushed by hand with a stainless steel mortar and pestle to a grain size of -35 mesh. The samples were then split with an aluminum microsplitter. They were split and mixed four times and then split until 100g portions remained. These portions were divided into three parts and mechanically pulverized to -200 mesh grain size in a ceramic ball mill for 15-20 minutes. The samples were placed in 6 dram glass bottles and homogenized by rotation on a mechanical wheel for 8-10 hours. Finally, the samples were dried in a 110°C oven for 12 hours to release any adsorbed water and then stored in a desiccator.

Preparation of fused glasses for XRF analysis

The fused glass disks for major and trace element analyses on the ER1XX samples were prepared using powdered sample and lithium-tetraborate flux. The flux was dried at 125° for 24 hours. Drying of the sample and flux is necessary to assure an exact flux:sample ratio, which is used to account for matrix corrections during the analysis. A ratio of 9:1 was chosen for optimum sensitivity and detection limits for the chosen elements.

Exactly 0.5000g of sample powder and exactly 4.5000g of flux were weighed into a glass vial. This mixture was then homogenized on a mechanical wheel for ten minutes. Longer mixing times created size fraction gradients along the sides of the vial. This changed the exact ratio of the mixture because the smaller particles of flux and sample tended to stick to the sides of the vial because of static.

The mixture was emptied into a 95% Pt-5% Au crucible and melted over a natural gas-air flame for 15-20 minutes until totally fluid and homogeneous in appearance. The melt was then poured into a 95% Pt-5% Au 3.25 cm pan which was heated to red hot by a natural gas-air flame. Heating the pan decreased the amount of air bubbles in the disk and allowed the melt to flow into the pan more easily.

The flame was removed immediately so as not to set up composition gradients within the disk.

The pan and disk were allowed to cool to room temperature and the disk was released from the pan by gently tapping it on its side. In this way nothing touched the analytical surface leaving a disk with no streaks and as few air bubbles as possible.

Care of the pan and crucible include handling only by Pt-tipped tongs when hot. The crucible was cleaned in a warm (80°) 6N HCl bath and rinsed in triple distilled water ($3XH_2O$). The pan was rinsed with 2N HCl and $3XH_2O$. The analytical surface of the pan was never touched by tongs or any other materials. As the pans were used they developed a bowed surface and since the analytical surface must be as flat as possible, the pans needed to be pressed in their original molds often.

Analysis of major and trace elements and loss on ignition

The major elements in the samples were analyzed using fused glass disks on a 3080E Rigaku XRF spectrometer at the Colorado School of Mines. Automated data reduction by regression analysis was obtained using the program S-MAX (Eriksson, 1986). Precision was determined by replicate analyses of all samples and is generally less than a range

of 2 percent except for K_2O and Na_2O (<10%) and P_2O_5 (<5%). Accuracy was determined to be greater than 99 percent by performing regression analysis for each oxide on 34 geochemical reference standards (Snyder, 1986; Eriksson, 1986).

The total iron in the samples was reported as Fe_2O_3 from the XRF analysis. The actual ratio of Fe^{2+} to Fe^{3+} is significant in determining the freshness of the sample and is useful in the modelling of mantle processes. Therefore, the iron as FeO was determined using a slightly modified wet chemical method of Goldich (1984).

Goldich chose to use pure quartz flasks to prevent contamination by elements contained in other types of glassware. Because of the expense and ultimate deterioration of quartz flasks by constant exposure to HF, we chose to use translucent F.E.P. Teflon flasks with screw on lids. Care must be taken not to overheat this type of flask because the bottom can begin to melt and make it difficult to determine if the sample has been totally dissolved. Also, screwing the cap on too tightly will cause a pressure build up during heating and may cause severe distortion of the flask. We had few problems producing a sufficient amount of heat to dissolve the samples without overheating the flasks.

Briefly, 0.5g of sample powder was weighed into a flask. The powder was dissolved by gently boiling in 5 ml of HF and 10 ml of H_2SO_4. After the sample was completely dissolved (~10 minutes), 50 ml of boric acid was added and the flask was cooled in a cold water bath. The mixture was then diluted to 125 ml with distilled water. The amount of Fe^{2+} in the sample was determined by titration with a standardized $KMnO_4$ solution. The amount of Fe_2O_3 reported was calculated by converting the total iron as Fe_2O_3 to total iron as FeO and subtracting the titrametrically determined FeO. The remaining value was then converted back to Fe_2O_3.

The trace elements Rb, Sr, Y, Nb and Zr were analyzed using loose powder in a 2 cm diameter plastic container covered with Mylar (Spex Industries) on a Kevex 5100 X-ray energy spectrometer at the USGS, BIG, in Denver. The precision and accuracy were determined to be less than 10 percent (Zel Peterman, personal communication).

The trace elements Co, Cr and V were determined using the same glass disks as for the major elements. The analyses were performed on a Rigaku 3070 XRF spectrometer at The Colorado College, Department of Geology, in Colorado Springs. The precision and accuracy of this method on a similar machine were estimated at less than 10 percent RSD

(Bower & Valentine, 1986; Bower, 1985).

Loss on ignition (LOI) was determined by gravimetric difference. Approximately 1g of powdered sample was weighed into a porcelain crucible and heated in a 1000°C muffle oven for 45 minutes. After heating, the crucible was placed in a desiccator and allowed to cool to room temperature. The difference in weights before and after heating gave the initial LOI. This value was converted to weight percent by dividing the initial LOI by the weight of the sample before heating and multiplying by 100. A loss of weight was reported as a positive LOI, but a weight gain was reported as a negative LOI. Because the heating did not take place in a vacuum, the oxidation of iron needed to be taken into account. During heating the Fe^{2+} is changed to Fe^{3+} and O_2 is added to the sample. This additional oxygen causes a significant change in the actual weight of the sample. To account for this oxidation, the weight of FeO in the sample, determined by titration, is multiplied by 0.111348. This number, added to the weight percent LOI, gave the actual LOI value of the sample.

Analysis of the rare earth elements

Analysis of the rare earth elements (REE) in the rock

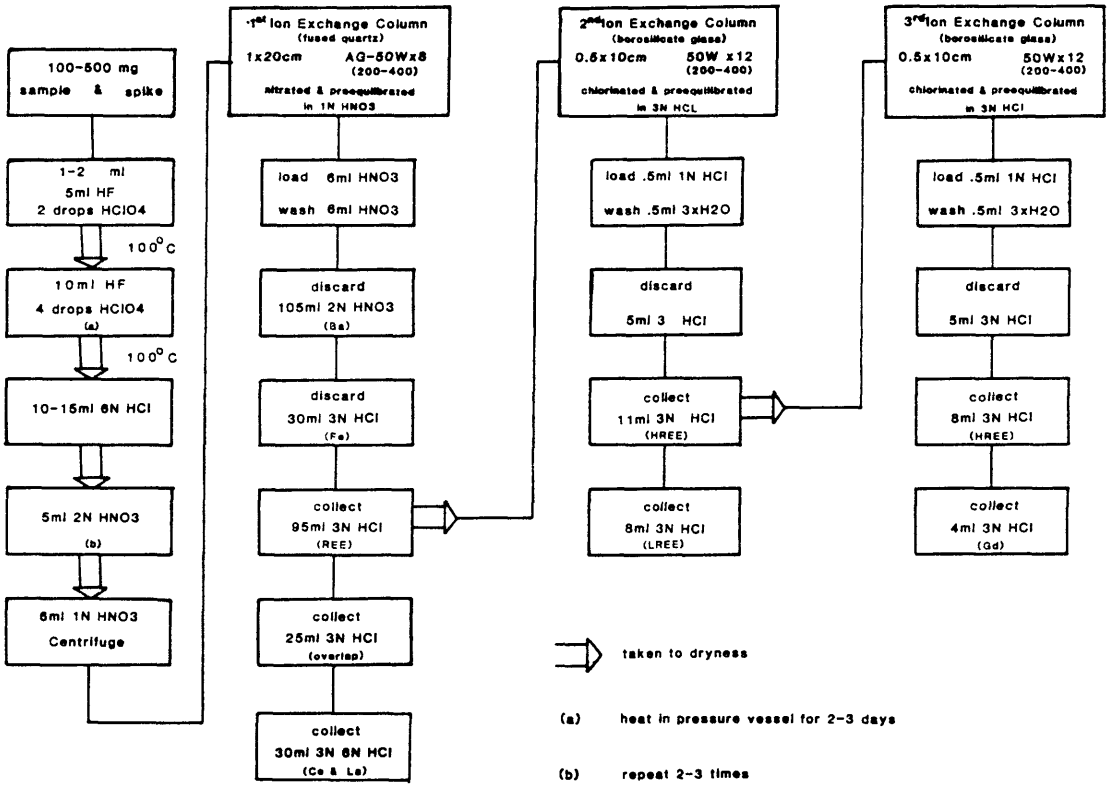

Figure IA.--Flow chart showing dissolution and separation procedures of rare earth elements.

samples was accomplished using isotope dilution mass spectrometry. This method was chosen so that the predicted low abundances of these elements in most samples could be determined with the greatest possible precision and accuracy. Figure IA is a flow diagram showing the dissolution and chemical separation procedures used to prepare these samples for analysis by mass spectrometry.

I. Sample Dissolution

Depending upon the estimated abundance of REE in the samples, from 100 to 500 mg of sample powder were weighed into acid-washed Savillex (brand) Teflon bombs. The powder was then wetted with 1 ml of 3XH_2O. From 100 to 500 mg of LREE and HREE spikes for isotope dilution were then added to the bombs. Rocks of komatiitic affinity are known to have low abundances of REE. Therefore, the sample:spike ratio was much larger for those rocks than for the other rocks of the suite.

One to 2 ml of HNO_3 was added to react with any organic material. Five ml of HF and two drops of $HClO_4$ were also added to the bombs. The bombs were left open and placed on a 100°C hot plate until they reached dryness. This allowed any initially dissolved silicon to be fumed off as SiF_4 gas.

Ten ml of HF and four drops of $HClO_4$ were added to the

bombs which were sealed and left on the hotplate for 2-3 days, depending upon the size and composition of the sample. When the samples were completely dissolved the bombs were opened and allowed to be heated to complete dryness (usually one day).

White residues are left after this point. They are brought into solution by the addition of 10-15 ml of 6N HCl. The bombs were sealed and placed on a 60°C hotplate. The isotope spike is allowed to come to total equilibrium with the entire dissolved sample. When this has been accomplished(~1 hour) the sample is again taken to dryness.

Because the chemical separation process begins with HNO_3, the sample residues were converted to nitrates by adding 2N HNO_3 and taking to dryness several times. This assures that no HCl is left in the residues which may change the elution rate. It is also important that no HF remain in the residue as it will etch the glassware used in the separation.

The samples are now ready to be loaded onto the elution columns for chemical separation of the REE. The residues are dissolved in 6 ml of 1N HNO_3 and transferred to Teflon test tubes. The mixtures are centrifuged to assure that all residue which does not dissolve remains

behind when the samples are loaded onto the columns. If residues are allowed in the columns they may slowly dissolve during the elution and destroy any separation of the elements and possibly cause contamination of other samples.

II. Separation chemistry for the REE

The separation scheme for the REE is a modification of that described by Lambert (1982). The initial separation began on a 1 x 20 cm glass column filled with AG-50WX8 (100-200 mesh) cation exchange resin equilibrated in 1N HNO_3. This resin is a different size than that originally used by Lambert (200-400 mesh) and affords a cleaner separation than the larger resin. This size column gives a clean separation and avoids overloading due to the large sample sizes used in this study (>100 mg). The separation of REE from the larger cations in the rock is greatly enhanced by a switch from HNO_3 to HCl. Adding a stronger concentration of HCl (6N) for the last part of the elution provides a clean separation of Ce and La from the rest of the REE. The elution curve for this procedure is shown in Fig. IB. The initial separation of the REE takes approximately 14 hours. Each of the subsequent separations (done as per Lambert, 1982) take 4-5 hours with 3 hours in between to clean the columns.

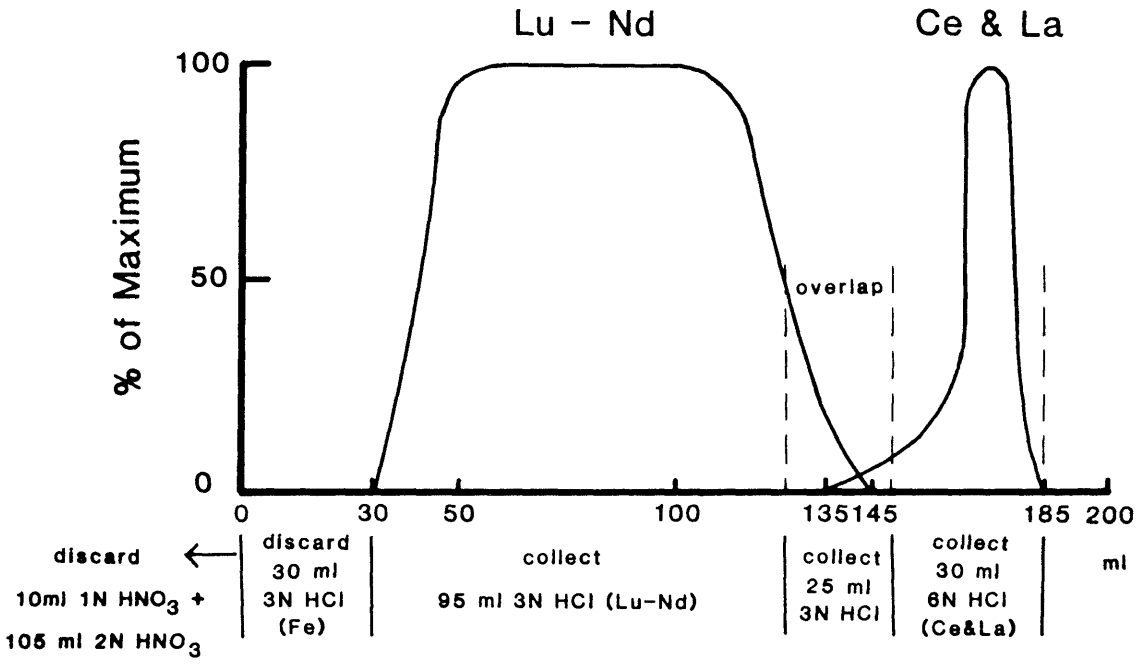

Figure IB.--Elution curve for the REE separation procedure.

III. Mass spectrometry

Isotope dilution analyses of the REE were performed on a 12" radius NBS Shields-type mass spectrometer at the USGS, BIG. The LREE and HREE were loaded as chlorides on Re-triple filaments and analyzed as ions. Gadolinium was loaded as a chloride on a Re-single filament and analyzed as an oxide.

Standard samples BCR-1 and BHVO-1 were analyzed and the results are listed in Table IA. A blank was also analyzed and negligible amounts of REE were found (Table IB).

For data interpretation, the analytical results were normalized to chondrite values (Table IC) in order to elminate irregularities in the patterns when the abundance was plotted against the element.

TABLE IA.

REE (ppm) in Standard samples BCR-1 and BHVO-1.

	BCR-1[1]	BCR-1[2]	BHVO-1[3]	BHVO-1[4]
Ce	53.5	53.9	39.7	36.7
Nd	28.9	28.8	24.5	23.4
Sm	6.65	6.57	6.09	5.79
Eu	1.97	1.97	2.08	2.00
Gd	---	6.64	6.26	6.01
Dy	6.40	6.34	5.14	4.95
Er	3.40	3.60	2.45	2.39
Yb	3.40	3.42	1.98	1.89

[1]Snyder (1986)
[2]Hanson (1980)
[3]this study
[4]Sun et al (1980)

TABLE IB.

REE (ug) in blank analysis.
(this study)

Ce	.0006
Nd	.0008
Sm	.0002
Eu	.0001
Gd	.0008
Dy	.0003
Er	----
Yb	.0001

TABLE IC.

Chondrite values used for normalization.
(Hanson, 1980)

Ce	.813
Nd	.597
Sm	.192
Eu	.0722
Gd	.259
Dy	.325
Er	.213
Yb	.208

APPENDIX II -- PETROGRAPHIC DESCRIPTIONS

Fine-grained mafic amphibolites (tholeiites):

(ER102, ER103, ER105, ER106, ER107, ER108, ER109, ER110, ER111, ER117)

These dark gray foliated rocks have segregation layering and schistosity which are apparent in both hand specimen and thin-section. All samples have a subidioblastic texture with grain sizes ranging from .05mm to 1mm for the major minerals. They are composed of approximately equal portions of amphibole and plagioclase with accessory sphene. Many also contain quartz. The amphiboles occur as prisms with ragged terminations and are either green hornblende, anthophyllite or both. Most amphibole grains have inclusions of quartz, plagioclase or opaques and many are twinned. The plagioclase composition ranges from An_{35} to An_{60} and occurs in equant xenoblastic grains, most of which are twinned. The sphene occurs as wedge-shaped crystals or drop-like granules less than .2mm in size. It often occurs in layers with the plagioclase and hornblende. Most samples also have accessory apatite. Opaques occur throughout the rocks but they have not been positively identified. Relative percentages and petrographic parameters of the minerals for each sample are listed in Table IIA. Significant deviation from or additions to the above description are listed below.

ER103: has opaques which occur in concentrated groups of euhedral crystals, often in a "star" pattern.
ER106: contains pyrite which is visible in hand specimen; opaques occur in layers with sphene.
ER107: contains ~1 percent biotite, .1mm to .2mm in length.
ER109: is an altered sample which contains epidote, sericite, chlorite and carbonate in quantities up to 3 percent; sericite and epidote have replaced some minerals along fractures and edges and along the twin planes in the plagioclase.
ER110: has a plagioclase content which is the most calcic of the suite, An_{60}.
ER111: has some of the plagioclase replaced by sericite and at least 50 percent is untwinned.
ER117: contains 1-2 percent euhedral hematite.

Coarse-grained mafic amphibolites (gabbros):

(ER114, ER116)

These rocks are similar in mineralogic composition to the fine-grained mafic rocks, although the texture of these rocks is extremely different. They are dark grey in color and do not have an obvious foliation. Segregation layering and schistosity are not apparent in hand specimen but there is a preferred orientation of amphibole prisms

in thin-section. The abundance of amphibole is much greater than that of plagioclase. The amphiboles (.05mm to 3mm in size) are green hornblende and cummingtonite. The plagioclase is andesine (An_{55-56}). Sample ER114 contains more plagioclase than ER116 which contains more cummingtonite. The amphiboles occur as compact clots, euhedral crystals or laths with ragged terminations which are surrounded by smaller grains of plagioclase and amphibole. There is a preferred orientation of the smaller grains around the larger grains. These larger amphibole grains contain euhedral inclusions of quartz or plagioclase. Sample ER114 also contains small (.05mm) subidioblastic quartz grains and a trace of hematite. Sample ER116 contains sphene and opaques in addition to the amphibole and plagioclase. Detailed petrographic parameters and mineral percentages are presented in Table IIA.

Fibrous ultramafic amphibolites (komatiites and komatiitic basalts):

(ER101a, ER101b, ER112, ER113, ER119, ER121, ER122)

These light to medium green fibrous rocks are composed mainly of tremolite/actinolite and chlorite. Most outcrops of these rocks are weathered black or rusty brown and most show some foliation. A few samples contain other types of amphibole. The amphiboles, which are .5mm to 2mm

in size, have only a slightly preferred orientation and many are twinned. The feathery textured chlorite does show a preferred orientation which is not necessarily the same as that of the amphiboles. All samples contain opaque minerals and iron oxide. Significant additions to or deviations from the above descriptions are listed below. Relative percentages and petrographic parameters are listed in Table IIA.

ER101a and ER101b: have tremolite grains which have darker pleochroic rims of actinolite.

ER112: contains only 2 percent chlorite but has Mg-anthophyllite, biotite and untwinned plagioclase; epidote alteration occurs along the boundaries between grains.

ER113: has a large percentage of opaque minerals (7-10 percent); most occur as shards which are concentrated in the cores of amphibole grains, most of which occur as prisms with ragged terminations.

ER119: is almost entirely composed of subidioblastic actinolite with only a trace of opaques and chlorite with no apparent alteration.

ER121: is an extremely altered sample which is severely fractured. These fractures are filled with epidote and some sericite.

Metasedimentary rocks:

ER104: is a fine- to medium-grained light grey rock with grain sizes ranging from .1mm to 1mm. It has a subidioblastic texture and is composed of 50 percent quartz, 30 percent labradorite plagioclase, 10 percent brown spotted biotite and 5 percent green hornblende with zircon and apatite as accessory minerals. The hornblende occurs intersertally with visible cleavage. The zircon and apatite are restricted to certain layers.

ER115: is a metaconglomerate having a fine-grained grey matrix with granophyric clasts up to 10 cm in length. The matrix is composed of fine-grained (.1mm to 1.5mm) quartz (50 percent), plagioclase (30 percent) and biotite (20 percent). The quartz has an idioblastic texture. The spotted biotite occurs as elongated prisms with olive green to light brown pleochroism and pleochroic halos around inclusions. The subidioblastic clasts are composed of larger (2-5mm) quartz grains (50 percent), orthoclase (30 percent) and mostly untwinned plagioclase. The plagioclase has a composition of An_{65}.

ER118: is a dark grey finely layered rock with no distinct schistosity or foliation. It has a subidioblastic texture with grain sizes ranging from .2mm to .5mm. There is a

faint lineation of the minerals in thin-section. It is composed of 35 percent dark blue-green hornblende, 25 percent quartz, 20 percent plagioclase (An_{55}), 10 percent almandine garnet and 7 percent black opaques with apatite and hematite as accessory minerals. The garnets are poikilitic with quartz inclusions elongated perpendicular to the lineation of the other minerals.

ER120: is a fine-grained (.1mm to .5mm) light grey rock with a wavy foliation. It is composed of 55 percent plagioclase (An_{54}), 25 percent quartz, 10 percent chlorite, 5 percent garnet, 5 percent sericite and 1-2 percent black opaques. The chlorite occurs as clots and are dispersed throughout the rock in a random manner. It has an abnormal purple interference color. The garnets have quartz inclusions and most are replaced by chlorite. Some patches are quite altered with sericite while the other areas are fairly fresh.

TABLE IIA.

Relative mineral percentages and petrographic parameters in mafic and ultramafic volcanic rocks from the Elmer's Rock Greenstone Belt.

Tholeiites

#	%Plag	An_x	2V	%hb	2V	ext<	%anth	2V	%qtz	%sph
ER102	35	49	-55	45	-55	16	15	+85	4	2
ER103	35	41	-55	35	-45	16	10	+80	15	-
ER105	25	42	+75	47	-85	17	7	-85	20	<1
ER106	45	38	+75	45	-60	17	--	--	<5	4
ER107	20	55	-60	50	+75	17	10	-85	15	tr
ER108	30	59	+60	45	-80	9	10	+83	10	3
ER109	30	58	+83	50	+75	17	--	--	<5	6
ER110	25	60	+50	30	-65	27	25	-85	10	4
ER111	25	58	+60	30	-47	9	25	-90	15	2
ER117	45	45	-60	30	-85	22	15	+85	--	5

Gabbros

#	%Plag	An_x	2V	%hb	2V	ext<	%cum	2V	ext<	Other
ER114	35	55	-40	30	-85	20	25	+75	19	10%qtz
ER116	15	56	+50	20	+60	16	60	+70	7	2%sph

Komatiitic rocks

#	%Trm/Act	2V	ext<	%Chl	%Opaq	Other
ER101a	60	-77	15	40	tr	
ER101b	95	-80	14	4	tr	
ER112	80	-87	23	2	--	5%plag 5%anth 2%bio
ER113	45	-77	15	10	10	35%cum
ER119	>99	-90	15	tr	tr	
ER121	15	-90	15	--	--	70%anth
ER122	>95	-85	14	4	tr	

Explanation:

plag = plagioclase
An_x = anorthite content
anth = anthophyllite
qtz = quartz
chl = chlorite
sph = sphene
hb =hornblende
cum = cummintonite
trm/act = tremolite/actinolite
opaq = opaque minerals

APPENDIX III -- MODEL CALCULATIONS*

TABLE IIIA.

Komatiitic rocks

	ER101b	ER122		ER113		
	(1)	(1)	(2)	(1)	(2)	(2)
C_o	chon*	chon*	101b	chon*	122	101b
$F=C_o/C_L$	.39	.04	.11	.01	.30	.03
D_o						
Ce	.01	.001	0	.001	0	0
Nd	.15	.006	-.044	.006	.15	.03
Sm	.15	.018	.051	.014	.32	.14
Eu	--	.024	--	.025	.53	.19
Gd	.16	.049	.23	.037	.49	.32
Dy	.25	.094	.36	.071	.78	.45
Er	.27	.130	.46	.110	.72	.55
Yb	.26	.150	.50	.130	.77	.60

(1) for partial melting $C_L/C_o=1/D(1-F)+F$

(2) for fractional crystallization $C_L/C_o=F^{(D-1)}$

(a) chondrite values (Hanson, 1980) except Ce=1.4xCHON, Nd=1.2xCHON

---

* The calulated values in these tables are used as examples of how model calulations work with these rocks. Specific models are discussed in the body of the thesis.

TABLE IIIB.

Tholeiitic rocks

Fractional crystallization: $C_L/C_o=F^{(D-1)}$

	ER105	ER110	ER102	ER117	ER107
C_o=(ER105)					
$F=C_o/C_L$	.91	.81	.50	.46	.79
C_L/C_o					
Ce	1.098	1.239	1.985	2.173	1.256
Nd	1.130	1.212	1.884	2.063	1.111
Sm	1.145	1.174	1.801	1.962	1.017
Eu	1.137	1.181	1.744	1.856	1.007
Gd	1.224	1.165	1.796	1.829	.990
Dy	1.166	1.033	1.603	1.598	.836
Er	1.163	.926	1.469	1.548	.721
Yb	1.171	.851	1.370	1.222	.636
D_o					
Ce	0	0	0	0	0
Nd	-.311	.104	.083	.067	.539
Sm	-.450	.251	.149	.131	.927
Eu	-.369	.223	.195	.203	.970
Gd	-1.16	.287	.152	.222	1.044
Dy	-.638	.850	.317	.396	1.784
Er	-.612	1.356	.442	.437	2.430
Yb	-.687	3.508	.544	.742	2.987

TABLE IIIB. (con't)

Partial melting: $C_L/C_o=1/D(1-F)+F$ $C_o=2xCHON$

	ER105	ER106	ER110	ER102	ER117	ER107
$F=C_o/C_L$	.19	.17	.15	.09	.08	.15
D_o						
Ce	.01	.01	.01	.01	.01	.01
Nd	.003	.049	.005	.010	.010	.024
Sm	.003	.046	.011	.015	.015	.043
Eu	--	.047	--	.019	.021	.044
Gd	.019	.046	.025	.024	.031	.064
Dy	.022	.061	.054	.040	.050	.111
Er	.029	.070	.089	.058	.059	.168
Yb	.023	.061	.106	.065	.094	.205

TABLE IIIC.

Mixing Model For ER107

Proportions of mixed liquids:[1] 26% komatiitic liquid
74% tholeiitic liquid

Element	komatiitic[2] composition	tholeiitic[3] composition	model[4] mixture	ER107
SiO_2 %	53.15	51.34	51.81	50.69
TiO_2	.49	.99	.86	.89
Al_2O_3	4.84	14.22	11.78	12.30
Fe_2O_3	.78	1.92	1.63	1.92
FeO	7.79	10.92	10.11	9.52
MnO	.10	.20	.17	.19
MgO	21.34	7.44	11.05	11.45
CaO	11.24	10.88	10.97	11.02
Na_2O	.15	1.75	1.33	1.69
K_2O	.06	.26	.21	.31
P_2O_5	.06	.09	.08	.08
Cr ppm	2072	218	663	713
Zr	40	50	48	49
V	136	299	260	282
Ratio				
$(Ce/Yb)_N$	1.33	1.00	1.04	1.08
$(Dy/Yb)_N$	1.38	1.18	1.23	1.32

---

1 determined using lever rule on Fig. 13.
2 average of ER101b & ER122
3 average of ER105 & ER106
4 X = .26(kom. liq.) + .74(thol. liq)

TABLE IIID.

Models For Cumulate Rocks.

Komatiitic rocks:

ER112

Model: adcumulate from komatiitic liquid

Normative mineralogy:
16.7% plag, 18.5% cpx, 62.3% opx[1]

$$D_o = \Sigma X_i Kd$$ [2]

Element	D_o	112/122[3]
Ce	.151	.069
Nd	.179	.116
Sm	.257	.167
Eu	.421	.314
Gd	.367	.227
Dy	.462	.310
Er	.540	.431
Yb	.664	.493

---

1 assuming all plag is cumulate and there is no trapped liquid
2 Kd's from Arth, 1976
3 assuming ER122 may be parental liquid

TABLE IIID. (con't)

ER119

Model: orthocumulate from komatiitic liquid

Normative mineralogy:
27.6% plag, 27.5% cpx, 32.1% opx, 9.4% ol
cumulate assemblage:
27.6% plag, 21.4% opx
intercumulus liquid:
10.7% opx, 27.5% cpx, 9.4% ol

$X_s = 48.5 \quad X_L = 51.5 \quad D_o = X_i Kd^2$

for X_L = 57% plag + 43% opx

$$C_L = \frac{C_R}{X_L + D_o(1-X_L)}$$

Element	D_o	C_L	$(C_L)_N$
Ce	.132	25.1	30.8
Nd	.105	13.3	22.2
Sm	.104	3.29	17.1
Eu	1.45	1.15	15.9
Gd	.111	3.80	14.7
Dy	.157	4.21	13.0
Er	.222	2.54	11.9
Yb	.307	2.45	11.8

---

1 assuming all plag is cumulate & cotectic proportions of plag and opx
2 Kd's from Schnetzler & Philpotts, 1970
3 C_R = measured concentration of i in the rock
4 chondrite normalized
5 interpolated between Sm & Gd

TABLE IIID. (con't)

Gabbros:

ER114, ER116

Model: ER114 (R2) residual liquid derived by fractional crystallization of some original liquid (C_o)
ER116 (R1) orthocumulate mixture of an adcumulate assemblage (C_a) & residual liquid (ER114)

$X_L = 0.25$[1] $\quad C_a = \frac{(R2) - X_L(R1)}{1 - X_L} \quad D_o = X_i Kd$

Major Elements	C_a	REE	$(C_a)_{N2}$	D_o3
SiO_2	46.35	Ce	3.45	.082
TiO_2	.53	Nd	3.41	.076
Al_2O_3	17.29	Sm	3.52	.086
FeO	10.53	Eu	5.26	.239
Fe_2O_3	-.05	Gd	3.33	.096
MnO	.24	Dy	3.41	.102
MgO	13.11	Er	3.53	.108
CaO	10.20	Yb	3.83	.114
Na_2O	1.71	C_a = 54.2% plag, 9.0% cpx		
K_2O	.10	5.1% opx, 30.5% ol		
P_2O_5	.04	Mg number = 68.9		

---

1 using Cr as the most depleted element (ie. all resides in liquid)
2 chondrite normalized
3 calculated for mass balance assemblage using Kd's from Arth, 1976